Stem Cell Reports
Article

ISSCR

OPEN ACCESS

A Novel GATA2 Protein Reporter Mouse Reveals Hematopoietic Progenitor Cell Types

Nouraiz Ahmed,[1] Leo Kunz,[1] Philipp S. Hoppe,[1] Dirk Loeffler,[1] Martin Etzrodt,[1] Germán Camargo Ortega,[1] Oliver Hilsenbeck,[1] Konstantinos Anastassiadis,[2] and Timm Schroeder[1,*]

[1]Department of Biosystems Science & Engineering, ETH Zurich, Mattenstrasse 26, 4058 Basel, Switzerland
[2]Biotechnology Center, Technische Universität Dresden, Tatzberg 47-51, 01307 Dresden, Germany
*Correspondence: timm.schroeder@bsse.ethz.ch
https://doi.org/10.1016/j.stemcr.2020.06.008

SUMMARY

The transcription factor (TF) GATA2 plays a key role in organ development and cell fate control in the central nervous, urogenital, respiratory, and reproductive systems, and in primitive and definitive hematopoiesis. Here, we generate a knockin protein reporter mouse line expressing a GATA2VENUS fusion from the endogenous *Gata2* genomic locus, with correct expression and localization of GATA2-VENUS in different organs. GATA2VENUS expression is heterogeneous in different hematopoietic stem and progenitor cell populations (HSPCs), identifies functionally distinct subsets, and suggests a novel monocyte and mast cell lineage bifurcation point. GATA2 levels further correlate with proliferation and lineage outcome of hematopoietic progenitors. The GATA2VENUS mouse line improves the identification of specific live cell types during embryonic and adult development and will be crucial for analyzing GATA2 protein dynamics in TF networks.

INTRODUCTION

Establishment and maintenance of cell states in multicellular organisms is regulated by a complex interplay of transcription factors (TFs). TFs exert their effects by fine-tuning gene expression programs. They control key cellular processes, including cellular homeostasis, metabolism, cell-cycle control, and cell fate determination, dictating the differentiation and development of complex tissues and organs. Misregulation of these transcriptional programs lead to a broad range of diseases, including developmental disorders and cancer (Lee and Young, 2013; Spitz and Furlong, 2012).

The TF GATA2 serves as a crucial regulator for development and function of several organs, e.g., the central nervous system (Nardelli et al., 1999), urogenital (Khandekar et al., 2004; Zhou, 1998) and reproductive organs (Siggers et al., 2002), respiratory and auditory systems (Suzuki et al., 2006), endothelial cells (Minami et al., 2004), and adipose tissues (Tong et al., 2000, 2005). Tissue-specific knockout of *Gata2* leads to a reduction in number of thyrotropes suggesting its role in cell fate determination of pituitary glands as well (Charles et al., 2006; Dasen et al., 1999). GATA2 is also required for trophoblast differentiation and correct functioning of placenta (Ray et al., 2009).

GATA2 has a prominent role in hematopoiesis where it has been shown to be indispensable to the development of primitive and definitive hematopoiesis (Bresnick et al., 2010, 2005; Shimizu and Yamamoto, 2005). *Gata2*-null mouse embryos fail to survive beyond embryonic day 10–11 (E10–E11), due to severe anemia. *Gata2*-null embryonic stem cells (ESCs) display a deficit in definitive hematopoiesis owing to limited expansion of hematopoietic colonies (Tsai et al., 1994). Adult *Gata2*$^{+/-}$ hematopoietic stem cells (HSCs) exhibit a reduced reconstitution capacity in competitive transplantation assays (Ling et al., 2004; Rodrigues et al., 2005). In contrast, HSCs with increased GATA2 levels fail to contribute to multilineage hematopoietic reconstitution of transplanted mice (Persons et al., 1999). Together, this suggests a GATA2 dose-dependent regulation of hematopoiesis.

GATA2 positively reinforces mast cell and basophil differentiation (Cantor et al., 2008; Kauts et al., 2018; Li et al., 2015; Ohmori et al., 2012, 2015) and its downregulation enables the proper transition of hematopoietic progenitor cells into the megakaryocyte and erythrocyte lineage through the GATA2–GATA1 switch mechanism (Bresnick et al., 2010; Doré et al., 2012; Grass et al., 2003; Snow et al., 2011).

Hence, it is becoming increasingly evident that correct GATA2 levels are crucial in regulating and maintaining the pool and function of many cell types in different organs. However, quantitative measurements of GATA2 protein levels are often still missing. Also, little is known about its precise molecular regulation, and how its protein levels relate to future functional outcomes. Understanding the GATA2 protein concentrations in diverse living cell types will provide insights into the role and regulation of GATA2 in different tissues.

One main reason is the lack of a reporter mouse line that can accurately reflect the endogenous GATA2 protein levels in different tissues. Suzuki et al. (2006) generated a mutant mouse line with a knockin of a green fluorescent protein (GFP) gene followed by a poly(A) sequence into the first exon of *Gata2* (Suzuki et al., 2006). This mouse line reports

the transcriptional activity, not protein levels, of the *Gata2* gene. Also, GFP fluorescence was restricted to only neural and hematopoietic cells and not present in other GATA2-expressing tissues. In addition, GFP has several drawbacks for imaging and multiplexing. Its overlapping emission spectrum prevents simultaneous use of cyan and yellow fluorescent proteins, and its excitation and emission spectra lead to high autofluorescence and low tissue penetrance (Okita et al., 2004). Recently, Kaimakis et al. (2016) generated a reporter for *Gata2* mRNA by inserting an IRES-VENUS cassette in its 3′ UTR. VENUS has a higher relative fluorescence intensity, is less pH sensitive, and matures faster than eGFP and hence is better for live imaging of biological samples (Nagai et al., 2002; Okita et al., 2004). However, the IRES-VENUS reporter also does not report GATA2 protein, but only mRNA, levels (Kaimakis et al., 2016; Eich et al., 2018) and with differing stability of the endogenous GATA2 and VENUS reporter proteins.

Here, we generate the first reporter mouse line for the non-invasive quantification of GATA2 protein levels by an in-frame knockin of VENUS FP into the C terminus of the *Gata2* genomic locus. These reporter mice are phenotypically normal, allow detection of heterogeneous GATA2 protein expression in different tissues during embryonic and adult development, and the identification, e.g., of novel hematopoietic stem and progenitor cell (HSPC) types, with distinct molecular and functional properties.

RESULTS

Generation of a GATA2VENUS Protein Reporter Mouse Line

We generated a novel reporter mouse line with a linker and VENUS fluorescent protein reading frame knocked into the gene locus of *Gata2* (Figures 1A and S1). VENUS was fused to the C terminus of GATA2 in exon 6, enabling the non-invasive quantification of GATA2 protein levels in all expressing cell types.

To exclude the possible alteration of GATA2 function, stability, or expression due to the VENUS fusion, we first confirmed the absence of abnormal phenotypes in homozygous GATA2VENUS mice. As described previously, *Gata2* deletion leads to embryonic lethality at the E10–E11 stage (Tsai et al., 1994), while altered expression levels result in a change, e.g., of the number and function of HSCs (Ling et al., 2004; Rodrigues et al., 2005; Persons et al., 1999). In contrast, homozygous GATA2VENUS mice showed no aberrant phenotype (Figures 1 and 2), were fertile and born at normal Mendelian ratios (Figure S2), and did not show increased mortality throughout adulthood (not shown). While altered GATA2 expression levels changes the composition of the HSPC pool (Kaimakis et al., 2016; Ling et al., 2004; Persons et al., 1999; Rodrigues et al., 2005), the frequencies of blood cells and HSPCs in bone marrow and peripheral blood from adult GATA2VENUS mice were unchanged (Figures 1B–1G and S3), and *in vitro* colony numbers (not shown) and types (Figures 1H and 1I) from GATA2VENUS HSCs were unaltered.

Quantitative immunostaining against GATA2 did not show any changed expression levels (Figure 1J) or stability (Figure 1L) of the GATA2VENUS fusion in different hematopoietic cell types. Simultaneous quantitative immunostaining against GATA2 and VENUS demonstrated their high correlation of expression and localization in HSPC nuclei (Figures 1K and S4). Thus, the GATA2VENUS fusion does not alter GATA2 function, stability, or localization, and can be used as a reliable readout of GATA2 protein expression.

GATA2VENUS Expression in Embryonic and Adult Organs

In addition to the hematopoietic system, GATA2 is expressed in numerous solid organs during embryonic development and in the adult (Charles et al., 2006; Dasen et al., 1999; Khandekar et al., 2004; Minami et al., 2004; Nardelli et al., 1999; Siggers et al., 2002; Suzuki et al., 2006; Tong et al., 2005, 2000; Zhou, 1998). Here, to analyze GATA2 expression in non-hematopoietic tissues, we established *in situ* immunostaining of GATA2 in various embryonic and adult organs. As expected (Charles et al., 2006; Dasen et al., 1999; Khandekar et al., 2004; Minami et al., 2004; Nardelli et al., 1999; Siggers et al., 2002; Suzuki et al., 2006; Tong et al., 2005, 2000; Zhou, 1998), GATA2 and GATA2VENUS expression was predominant in the embryonic nasal cavity, inner ear, ventral mid brain, urogenital system (Figures 2A–2E), and in the adult mouse kidney (Figures 2F and 2G). Co-immunostaining against GATA2 and VENUS in different organs confirmed colocalization of GATA2 and VENUS signal in nuclei, demonstrating normal GATA2VENUS localization (Figure 2). Thus, the GATA2VENUS mouse line is a faithful reporter of GATA2 protein expression in different tissues.

Heterogeneous GATA2 Expression in Adult HSPCs

To date, GATA2 expression is largely analyzed at the RNA level. Its protein expression was only quantified in developmental hematopoiesis or by using population average biochemical assays, masking GATA2 protein levels and heterogeneity at the single-cell level and thus hampering our understanding of GATA2 regulation and function during HSC differentiation (Etzrodt et al., 2014; Hoppe et al., 2014). Here, we profiled the single-cell expression of GATA2 protein in 20 adult HSPC populations encompassing the whole myeloid lineage, including the erythrocyte, megakaryocyte, mast cell, basophil, eosinophil, neutrophil, and monocyte lineages (Figures 3, S3, and S5).

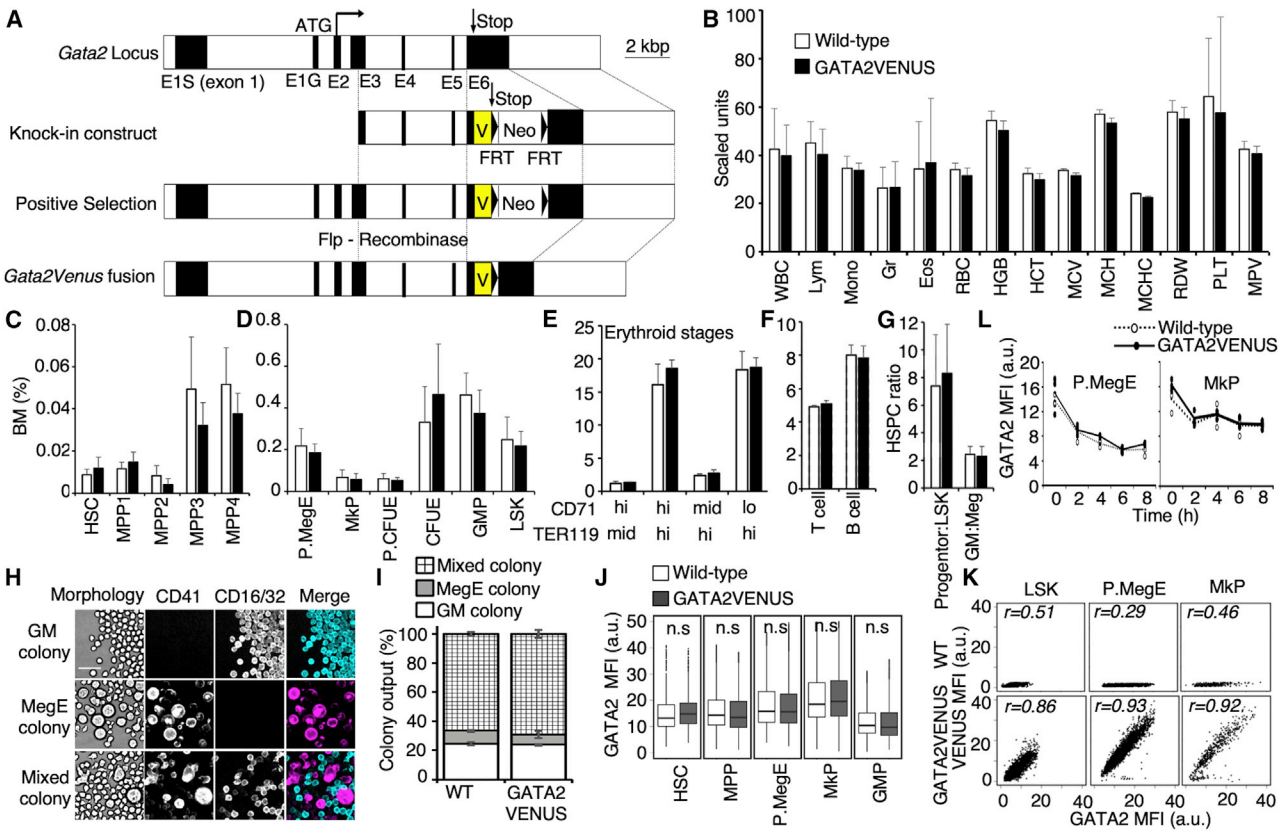

Figure 1. Generation of a GATA2VENUS Knockin Protein Reporter Mouse Line with Normal Hematopoiesis

(A) Constructs used for GATA2VENUS knockin generation. The *FRT PGK-Neo FRT* was deleted by cross with a Flpe deleter mouse line. Black boxes indicate exons (also see Figure S1).

(B) Peripheral blood counts are not altered in GATA2VENUS mouse line. WBC, white blood cells (200 cells per mm^3); Lym, percent lymphocytes of WBC (%); Mono, percent monocytes of WBC (0.1%); Gr, percent granulocytes of WBC (%); Eos, percent eosinophils of WBC (0.2%); RBC, red blood cells (2×10^5 cells per mm^3); HGB, hemoglobin (0.2 g/dL); HCT, hematocrit (%); MCV, mean corpuscular volume (μm^3); MCH, mean corpuscular hemoglobin (0.2 pg); MCHC, mean corpuscular hemoglobin concentration (g/dL); RDW, red cell distribution width (0.2%); PLT, platelets (10^4 per mm^3); MPV, mean platelet volume (0.1 μm^3) (n = 9 mice per genotype).

(C–G) Fusion of VENUS to GATA2 does not alter bone marrow composition. Data indicate bone marrow percentage of (C) HSCs and multipotent progenitors (n = 7 mice per genotype), (D) lineage committed progenitors (n = 10 mice per genotype), (E) early and late erythrocyte progenitors (n = 3 mice per genotype), (F) T and B cells (n = 3 mice per genotype), and (G) ratio of multipotent progenitors to lineage committed progenitors and granulocyte-monocyte progenitors to megakaryocyte-erythrocyte (MegE) progenitors (n = 10 mice per genotype).

(H and I) Colony-forming potential and output of HSCs is not altered in GATA2VENUS mouse line. (H) Single HSCs sorted into 384-wells in IMDM, FCS, BIT, SCF, EPO, TPO, IL-3, and IL-6. Granulocyte-monocyte (GM) colonies identified by morphology and FCγR expression. MegE colonies identified by morphology and CD41 expression. Scale bar, 50 μm. (I) Types of colonies formed from HSCs (n = 3 independent mice per genotype).

(J) Protein levels of GATA2 are not altered in different cell types in GATA2VENUS mouse line. Data were acquired using quantitative immunostaining against endogenous GATA2 protein. Data represented by box and whisker plots with median of GATA2 intensity (n = 3 independent mice per genotype).

(K) Endogenous GATA2 protein levels correlate to VENUS fusion levels. Data were acquired using quantitative immunostaining against GATA2 and VENUS and represented by a 2D plot of GATA2 and VENUS intensities. Number (r) in the plots indicate Pearson correlation coefficient (n = 3 independent mice per genotype).

(L) Normal stability of GATA2 fusion proteins in pre-MegE progenitors (preMegEs) (left panel) and megakaryocyte progenitors (MkPs) (right panel). Data were acquired using quantitative immunostaining against GATA2 in indicated cell types after treatment with 50 μM cycloheximide (protein translation inhibitor) and sampling of cells at the indicated time points (n = 3 independent mice per genotype). Error bars in (B)–(G) and (I) = SD. Data in (J)–(L) indicate mean fluorescence intensity (MFI) of GATA2 and VENUS. Difference between wild-type and GATA2VENUS samples is non-significant unless specified. Two-sample t test; ***$p < 0.001$, **$p < 0.01$, *$p < 0.05$.

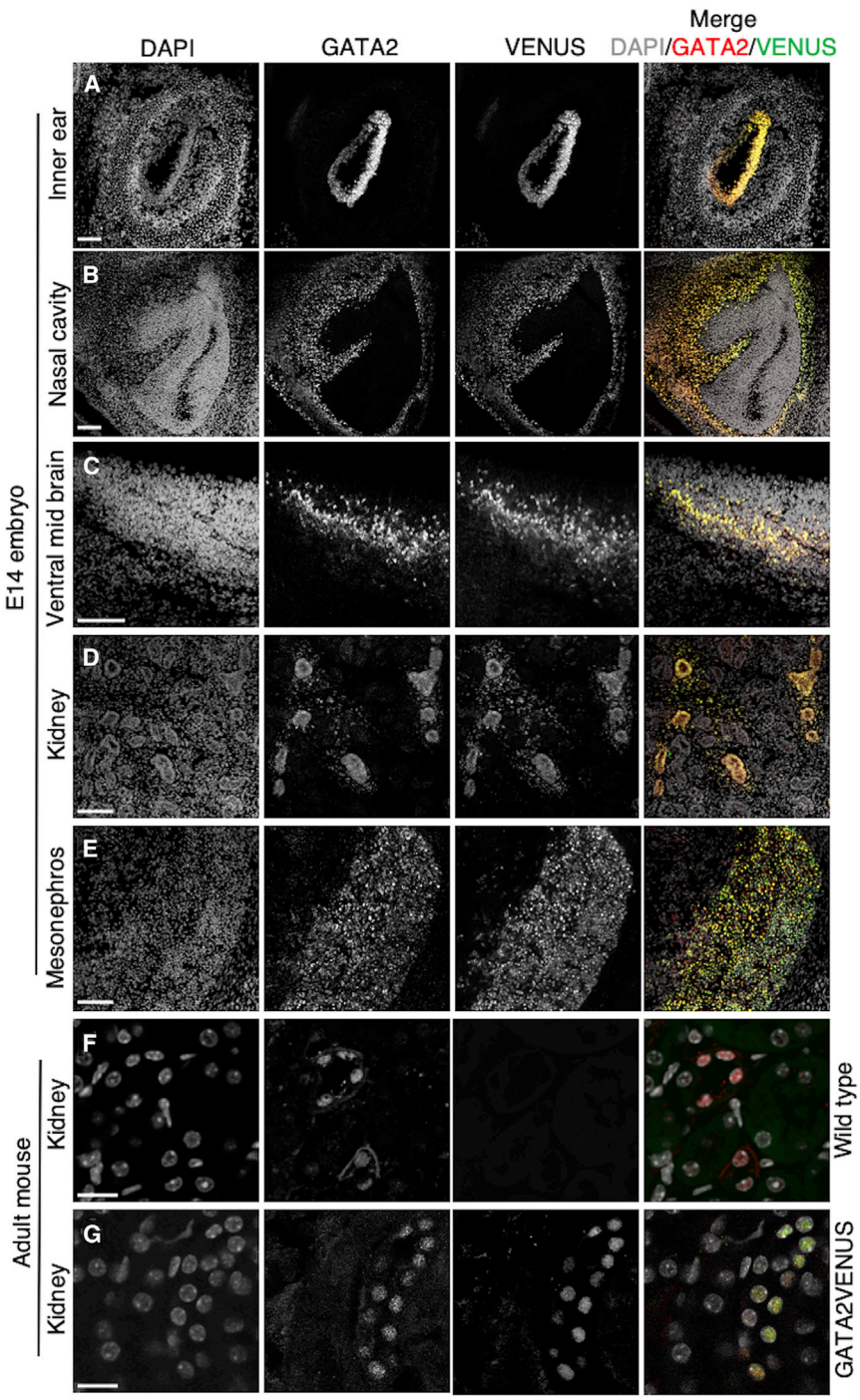

Figure 2. Normal Expression and Localization of GATA2VENUS in Embryonic and Adult Tissues

Localization of GATA2VENUS is similar to GATA2 in nuclei of the inner ear (A), nasal cavity (B), ventral mesoderm (C), kidney (D), and mesonephros (E) from E14 embryo and kidney from adult wild-type (F) and GATA2VENUS (G) mice. Confocal images of E14 embryo (A–E) and 12-week-old adult mouse (F–G) sections stained with DAPI (nuclei), and anti-GATA2 and anti-GFP antibodies. Scale bars, 100 μm (A–E) and 10 μm (F–G).

GATA2 is homogeneously expressed at low level in long-term HSCs , and heterogeneously in different MPP populations (Cabezas-Wallscheid et al., 2014; Wilson et al., 2008). Of all the populations analyzed, pre-megakaryocyte-erythrocyte progenitors (Pronk et al., 2007), megakaryocyte progenitors (Pronk et al., 2007), mast cell progenitors (Chen et al., 2005), and basophil progenitors (Arinobu et al., 2005) exhibit the highest expression of GATA2. In contrast, monocyte progenitors (MPs) (Yanez et al., 2017) and monocyte dendritic cell progenitors (Hettinger et al., 2013) show lowest expression of GATA2. GATA2 is downregulated from the $CD71^{high}$ $TER119^{low}$ to the $CD71^{low}$ $TER119^{high}$ stage (Pop et al., 2010), in line with the proposed GATA2 downregulation during

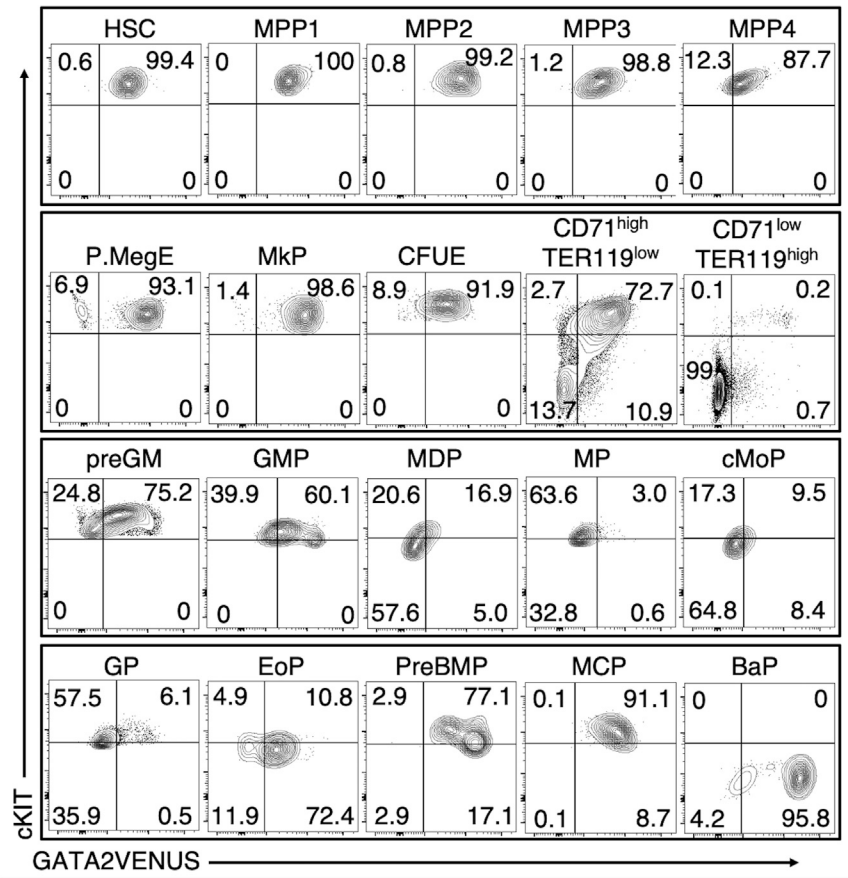

Figure 3. Cell-Type-Specific and Heterogeneous GATA2 Protein Expression in Adult HSPCs

Flow-cytometric quantification of GATA2-VENUS expression in adult HSPCs. GATA2-VENUS gate was set using wild-type cells (see Figure S5). Numbers in quadrants represent percentage of cells. See Figure S3 for gating schemes for these cell types: HSC, hematopoietic stem cell; MPP 1–4, multipotent progenitors 1–4; P.MegE, pre-megakaryocyte-erythrocyte; MkP, megakaryocyte progenitor; CFUE, colony-forming unit erythrocyte; $CD71^{high}TER119^{low}$ and $CD71^{low}TER119^{high}$, erythrocyte differentiation stages; preGM, pre-granulocyte-monocyte; GMP, granulocyte-monocyte progenitor; MDP, monocyte dendritic cell progenitor; MP, monocyte progenitor; cMoP, common monocyte progenitor; GP, granulocyte progenitor; EoP, eosinophil progenitor; preBMP, pre-basophil mast cell progenitor; MCP, mast cell progenitor; BaP, basophil progenitor.

erythrocyte differentiation (Bresnick et al., 2010; Doré et al., 2012; Grass et al., 2003; Snow et al., 2011) (Figures 3, S3, and S5).

Interestingly, we also observed large heterogeneity of GATA2 expression in the pre-granulocyte-monocyte progenitor (preGM) and granulocyte-monocyte progenitor (GMP) (Pronk et al., 2007) populations (Figure 3), indicating novel GATA2-based subpopulations. This is reminiscent of previous studies highlighting heterogeneous GATA1 expression in preGMs and GMPs (Drissen et al., 2016; Hoppe et al., 2016).

GATA2 Protein Expression Identifies HSPC Subsets with Distinct TF Networks

The heterogeneous GATA2 expression in preGMs and GMPs suggested the existence of subtypes with specific molecular and functional properties. To analyze this further in a quantitative way, we used a simple, robust, and efficient multiplexed immunostaining protocol. It has high enough throughput and sensitivity to work with rare cell types and permits automated imaging and multiplexed single-cell TF protein quantification in primary HSPCs. In addition, it is quantitative enough to detect minor variations in TF levels (Figures 4B and 4C).

We quantified the protein expression of core hematopoietic TFs in freshly sorted GATA2-negative and -high preGMs and GMPs (Figure 4A). GATA2-negative preGMs and GMPs showed no GATA1 and FOG-1 expression, whereas GATA2 -high preGMs and GMPs showed high expression. IRF8, a monocyte and dendritic cell marker, displayed an inverse pattern of expression, with high IRF8 expression in GATA2-negative cells. No or only minor correlations of PU.1 and CEBPα with GATA2 expression could be observed, despite a >2-fold increase in CEBPα expression during preGM to GMP transition (Figures 4B and 4C).

Thus, the GATA2VENUS mouse line enables identification of HSPC subsets with distinct TF networks within populations previously assumed to be homogeneous and allows better understanding of molecular pathways regulating hematopoietic cell fate.

GATA2 Expression Identifies Early Segregation of Monocyte and Mast Cell Lineages

TF networks determine cell fate of HSPCs (Krumsiek et al., 2011). The differential expression of core hematopoietic

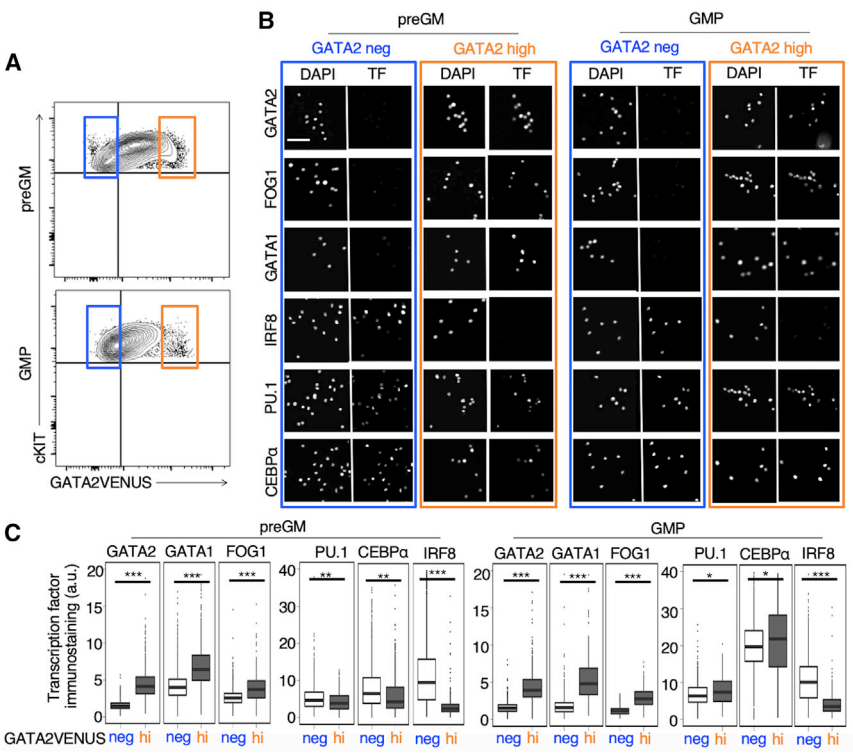

Figure 4. GATA2 Protein Expression Identifies preGM and GMP Subpopulations with Differential Hematopoietic TF Expression

(A) GATA2-negative and -high preGMs and GMPs were sorted before immunostaining, imaging, and quantification of core hematopoietic TFs.

(B) Representative fluorescence images of preGMs (left panel) and GMPs (right panel) stained with DAPI and anti-TF antibodies. Scale bar: 50 μm.

(C) Quantification of TF levels in GATA2-negative and -high preGMs and GMPs. Data represented by box and whisker plots with median (n = 3 independent mice). Two-tailed t test; ***p < 0.001, **p < 0.01, *p < 0.05.

TFs, such as GATA1, FOG1, and IRF8 in heterogeneous preGMs and GMPs suggests distinct differentiation potentials.

To determine whether GATA2 expression can identify HSPC subsets with different lineage potential, we cultured freshly sorted GATA2-negative and -high preGMs and GMPs under pan-myeloid conditions (Dahlin et al., 2018; Drissen et al., 2016) (with cytokines stem cell factor, interleukin-3 [IL-3], IL-9, and granulocyte-monocyte colony-stimulating factor [GM-CSF]) for 8 days and quantified the resulting cultures by morphology and molecular markers (Figures 5A and S6). Morphological analysis indicated that GATA2-negative versus -high progenitors predominantly generated monocytes and macrophages, versus mast cells, respectively. In contrast, neutrophils were generated from both progenitors, albeit with lower frequency from GATA2-high progenitors (Figure 5C). Consistent with the morphological observations, flow cytometry of GATA2-high cultures revealed a high frequency of cKIT$^+$ FCεR1$^+$ mast cells with no CD115 expression, and some CD11b$^+$ LY6G$^+$ neutrophils. In contrast, GATA2-negative progenitors mostly produced CD11b$^+$ CD115$^+$ monocytes and CD11b$^+$ LY6G$^+$ neutrophils and no mast cells (Figure 5B).

Thus, GATA2 expression in preGM and GMP populations identifies cells with mast cell commitment (Ohmori et al., 2015) and demonstrates early segregation of monocyte and mast cell lineages, but not neutrophils, before the preGM and GMP stage.

GATA2 Protein Levels Predict preGM and GMP Proliferation and Lineage Potential

Next, we analyzed if the expression levels of GATA2 protein in preGMs and GMPs can predict their proliferation and lineage potential. We single-cell-sorted preGM and GMP populations into negative, low, mid, and high GATA2 expressers, and cultured them under pan-myeloid conditions (Dahlin et al., 2018; Drissen et al., 2016) (Figure 6).

Fluorescent antibodies against surface markers CD115, LY6G, and FCεR1 were added to live colonies to identify monocytes, neutrophils, and mast cells, respectively (Eilken et al., 2011, 2009). After 8 days, we observed different colonies, including unipotent (monocyte, neutrophil, and mast cell), bipotent (monocyte-neutrophil and mast cell-neutrophil), and extremely rare tripotent (monocyte-neutrophil-mast cell) colonies (Figure 6A). Unipotent monocyte colonies were exclusively generated from GATA2-negative preGMs and GMPs, while unipotent mast cell colonies were exclusively generated from GATA2 higher progenitors. GATA2-low and -mid cells predominantly generated bipotent colonies, including monocyte-neutrophil and mast cell-neutrophil colonies. These results hence rule out the existence of a bipotent monocyte-mast cell progenitor (Figure 6D). Interestingly,

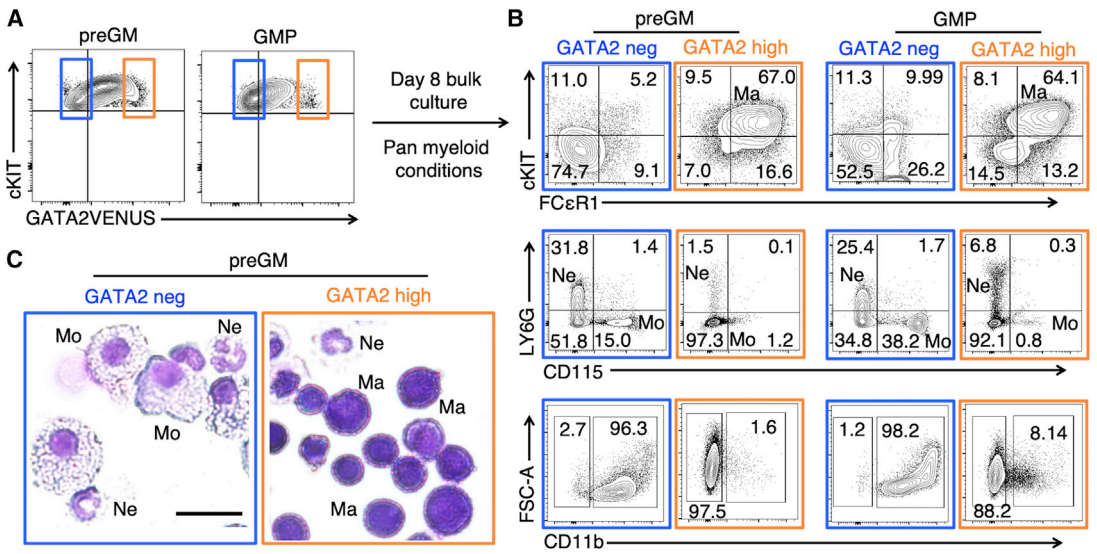

Figure 5. GATA2 Protein Levels Identify Early Segregation of Monocyte and Mast Cell Lineages but Not Neutrophils

(A) GATA2-negative and -high preGMs and GMPs were sorted and cultured in pan-myeloid medium (IMDM + FCS + BIT + SCF + GM-CSF + IL-3 + IL-9).

(B) Quantification of mature cell types at day 8 by flow cytometry. GATA2-negative preGMs and GMPs mainly generate $CD11b^{+}$ $CD115^{+}$ $FC\varepsilon R1^{-}$ monocytes and $CD11b^{+}$ $LY6G^{+}$ $FC\varepsilon R1^{-}$ neutrophils while GATA2-high preGMs and GMPs generate $cKIT^{+}$ $FC\varepsilon R1^{+}$ $CD11b^{-}$ $CD115^{-}$ $LY6G^{-}$ mast cells and few neutrophils. Numbers in quadrants represent percentage of cells.

(C) Representative images of May-Grünwald Giemsa morphology of cells from day 8 culture preGMs. GATA2-negative versus -high preGMs generate monocytes and neutrophils versus mast cells and neutrophils, respectively. Scale bar, 20 μm.

GATA2-low and -mid preGMs generated colonies with higher numbers of cells than GATA2-negative or -high preGMs (Figure 6C). These data establish low GATA2 protein levels as a marker of unipotent monocyte and high GATA2 protein levels as a marker for mast cell progenitors. Thus, specific GATA2 protein expression levels identify and possibly regulate distinct proliferation and lineage potentials for early myeloid progenitors.

DISCUSSION

GATA2 TF has long been known as a crucial regulator of the development, differentiation, and function of numerous tissues, including the central nervous system, pituitary glands, adipose tissues, endothelial cells, and urogenital and reproductive systems (Charles et al., 2006; Dasen et al., 1999; Khandekar et al., 2004; Minami et al., 2004; Nardelli et al., 1999; Siggers et al., 2002; Tong et al., 2005, 2000; Zhou, 1998). A prominent role of GATA2 in regulating the emergence, maintenance, function, and differentiation of HSCs, both during embryonic and adult phases of definitive hematopoiesis, has been well documented (de Pater et al., 2013; Gao et al., 2013; Kaimakis et al., 2016). Correct GATA2 expression levels are required for the normal development of numerous cell types (Ling et al., 2004; Persons et al., 1999; Rodrigues et al., 2005).

However, little is known about the precise protein levels and molecular regulation of GATA2 protein and how this relates to the functional outcome during cell fate determination and development of different organs. To better quantify the heterogeneity and dynamics of TFs, such as GATA2, which play a crucial role in regulating, e.g., hematopoietic lineage choice (Etzrodt et al., 2014; Hoppe et al., 2014; Loeffler and Schroeder, 2019; McIvor et al., 2003; Schroeder, 2005), requires reporter mice enabling the non-invasive quantification of their protein levels at the single-cell level (Etzrodt and Schroeder, 2017), e.g., by TF-fluorescent protein fusion reporters. Since these fusions could potentially change the TF's function or stability, the absence of these changes has to be confirmed before further using them (Filipczyk et al., 2015; Hoppe et al., 2016).

Here, we therefore generated a GATA2VENUS knockin protein reporter mouse line. Although *Gata2*-null embryos are non-viable (Tsai et al., 1994), have severe deformations of the urogenital system (Khandekar et al., 2004; Zhou, 1998), and GATA2-haploinsufficiency results in altered hematopoiesis (Ling et al., 2004; Rodrigues et al., 2005), homozygous GATA2VENUS mice are normal, without urogenital deformations, fertile, and born at expected Mendelian frequencies. GATA2VENUS has normal protein stability, and the same expression as GATA2 across different cell types. While even minor changes in GATA2 expression

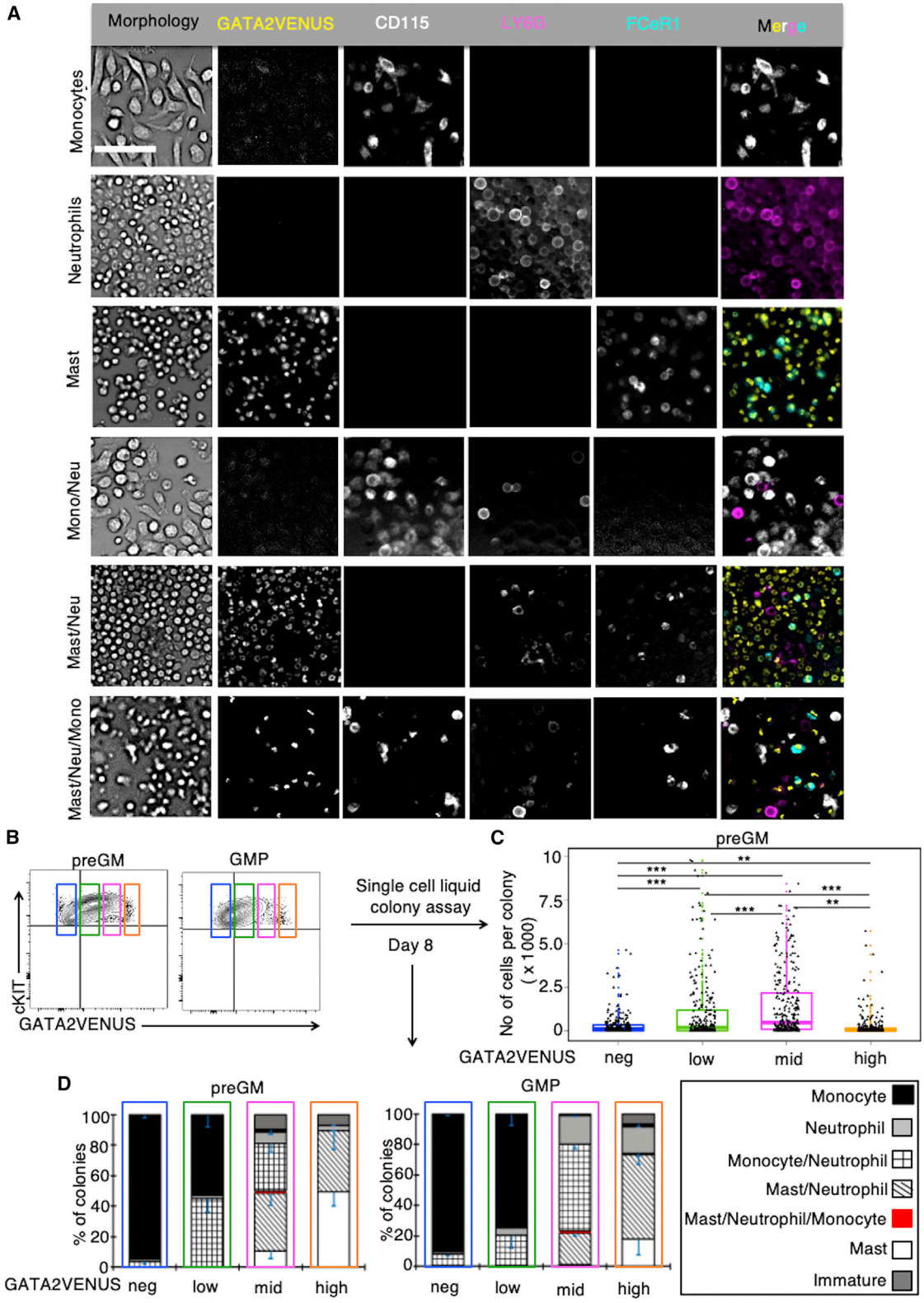

(legend on next page)

levels lead to changed HSPC pool sizes (Ling et al., 2004; Rodrigues et al., 2005), we could not detect changes in hematopoiesis or the morphology of other organs expressing GATA2 in homozygous GATA2VENUS mice. Thus, the GATA2VENUS fusion does not change GATA2 function, stability, or expression.

Although previous studies highlighted the expression of GATA2 in different organs, the correlation of GATA2 protein levels and function in regulating the development and homeostasis of these organs is not well understood. Therefore, the produced reporter line can be used to better analyze the role of GATA2 in the many live tissues during embryonic and adult development stages where it is expressed and functionally important. These include, for example, motor neuron precursors and the olfactory bulb in the embryonic central nervous system (Nardelli et al., 1999), epithelium of developing ureteric buds destined to become collecting tubules of kidney (Khandekar et al., 2004; Zhou, 1998), and trophoblast cells covering the inner cell mass and blastocoel of developing embryo (Ray et al., 2009). The GATA2VENUS mouse can also aid in identifying and further characterizing the endothelial cells undergoing EHT during HSC generation at E10.5, all long-term repopulating HSCs and a large fraction of hematopoietic progenitors and erythromyeloid progenitors in mid-gestation embryo (Kaimakis et al., 2016; McGrath et al., 2015) and distinct erythroid differentiation stages in the fetal liver (Pop et al., 2010).

GATA2 protein expression in 20 different HSPC types showed unique patterns and heterogeneity in different populations suggesting distinct molecular pathways affecting, and regulated by, GATA2 expression. The observed GATA2 heterogeneity in preGMs and GMPs allowed identification of novel subtypes within these phenotypically identical (Akashi et al., 2000; Pronk et al., 2007) populations. Importantly, since GATA2 is expressed in all HSCs while many other TFs, such as GATA1, are expressed later in differentiation (Drissen et al., 2016; Hoppe et al., 2016), GATA2 is likely a central TF in the hematopoietic lineage decision TF network. The GATA2-GATA1 switch during erythrocyte differentiation (Bresnick et al., 2010; Doré et al., 2012; Grass et al., 2003; Snow et al., 2011), and the cooperation of GATA2 with PU.1 and CEBPα during the specification of mast cell and basophil lineages (Iwasaki et al., 2006; Ohmori et al., 2015; Walsh et al., 2002) are two examples of GATA2-controlled lineage choice. We have established a multiplexed immunostaining protocol and used it to screen core hematopoietic TFs in GATA2-negative and -high preGMs and GMPs. The observed high levels of GATA1 and FOG-1 expression in GATA2-high progenitors suggest distinct molecular programs in GATA2-negative and -high preGMs and GMPs with distinct potential. Indeed, GATA2-negative and -high preGM and GMP populations generate monocytes and mast cells, respectively. This is in line with a recent report on early segregation of monocyte and mast cell lineages using a GATA1 reporter mouse line (Drissen et al., 2016). The new reporter line allows to sort for monocyte and mast cell progenitors based on GATA2VENUS levels and therefore will aid their molecular characterization.

Despite homogeneous low GATA2 expression in HSCs, we find heterogeneity in GATA2 expression already in MPPs. Together with the segregation of monocyte and mast cell lineages with GATA2 expression at the preGM stage, this suggests monocyte-mast cell lineage bifurcation already at the preGM and likely MPP stage. This is in agreement with recent single-cell RNA sequencing analysis confirming heterogeneous MPP *Gata2* expression at the mRNA level (Weinreb et al., 2020). High *Gata2* mRNA-expressing MPPs (likely corresponding to GATA2 protein high MPP2 in our study) predominantly differentiated to the mast cells and the megakaryocyte-erythrocyte lineage, whereas Gata2-low MPPs (corresponding to GATA2-low MPP3 and 4 in our study) differentiated to monocytes and neutrophils, respectively. Altogether, this suggests lineage commitment at the MPP stage and thus earlier than previously thought. It suggests GATA2 as a potential regulator of this lineage choice (Figure 7) (Akashi et al., 2000; Cabezas-

Figure 6. Variations in GATA2 Protein Levels Correlate with HSPC Proliferation and Lineage Potential

(A) Quantification of liquid colonies from single preGMs or GMPs by quantitative imaging of cell morphology, nuclear shape, and expression of GATA2VENUS, CD115 (monocytes), LY6G (neutrophils), and FCεR1 (mast cells). Examples shown for monocyte, neutrophil, mast cell, bipotent monocyte-neutrophil, bipotent mast cell-neutrophil, and tripotent monocyte-neutrophil-mast cell colonies. Immature colonies do not express any surface markers. Scale bar, 50 μm.

(B) Four different preGM and GMP fractions based on GATA2 levels were single-cell sorted into 384-well plates and cultured for 8 days in pan-myeloid media (IMDM + FCS + BIT + SCF + GM-CSF + IL-3 + IL-9).

(C) GATA2 -low and -mid preGMs exhibit higher proliferation and colony-forming potential than GATA2 -negative and -high cells. Data represented by box and whisker plots with median. Dots indicate individual measurement per cell (n = 3 independent mice).

(D) GATA2 protein expression correlates with different preGM and GMP lineage potential. Mean percentage of different colony types identified in (A) (n = 3 independent mice). Error bars = SD. Number of colonies, preGMs: GATA2-neg, 155; GATA2-low, 225; GATA2-mid, 157; GATA2-high, 152. GMPs: GATA2-neg, 173; GATA2-low, 153; GATA2-mid, 161; GATA2-high, 91. Two-sided Wilcoxon rank-sum test; ***$p < 0.001$, **$p < 0.01$, *$p < 0.05$.

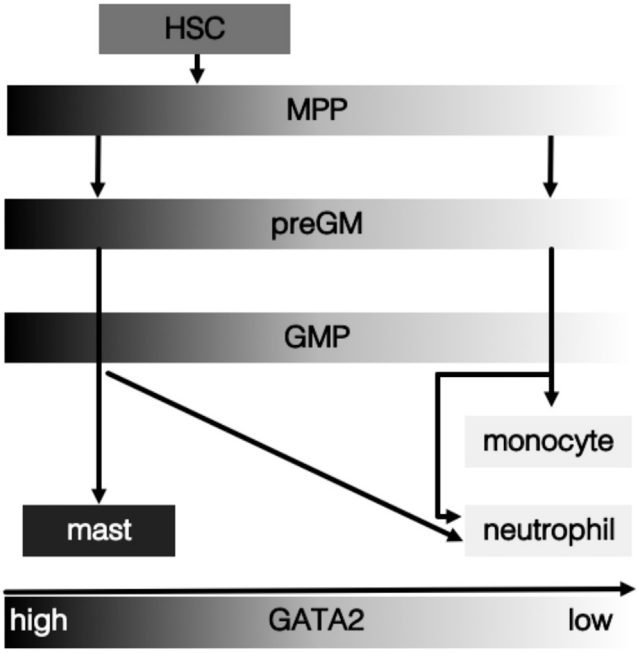

Figure 7. Early Segregation of Monocyte and Mast Cell Lineages
Based on GATA2 expression, monocyte, and mast cell lineages bifurcate already within the preGM and likely the MPP compartment. Neutrophil fate is shared between GATA2-low and -high pathways. Only mast, neutrophil, and monocyte lineages are shown. Infrequent transition between GATA2-low and -high states in MPPs, preGMs, and GMPs may be possible.

Wallscheid et al., 2014; Pietras et al., 2015; Pronk et al., 2007; Weinreb et al., 2020).

Concentrations of TFs regulate differentiation and developmental pathways. This includes, for example, the differentiation of HSCs toward GM lineage in response to above-threshold levels of PU.1 TF and the transition of fetal liver progenitors into B cells versus macrophages governed by relative concentration of PU.1 (Graf and Enver, 2009; Hoppe et al., 2016; Kueh et al., 2013). Indeed, sub-fractionation of preGMs and GMPs into four subsets based on GATA2 protein levels demonstrated high fractions of bipotent colonies with increased proliferation potential in GATA2-low and -mid progenitors compared with GATA2-negative and -high progenitors, which suggests that variations in GATA2 levels correlate to distinct proliferation and lineage potential. However, whether GATA2 levels are a cause or consequence of different functional outcomes is a matter of future interest.

It will be interesting to know how GATA2 levels and dynamics are involved in the lineage choice of early myeloid progenitors, its role in controlling the decision between mast cell and monocyte lineages, how the levels and dynamics of GATA2 modulate the onset of the GATA2-GATA1 switch, and if and how GATA2 regulates other master regulators of hematopoiesis, including PU.1 and CEBPα. In addition, the novel reporter line will be invaluable for better analyzing GATA2 regulation and function in many solid tissues it regulates.

EXPERIMENTAL PROCEDURES

Animals

Experiments were performed with 12- to 16-week-old wild-type, male C57BL/6J mice from Janvier Labs and in-house generated GATA2VENUS reporter mice. Animal experiments were approved according to Institutional guidelines of ETH Zurich and Swiss Federal Law by veterinary office of Canton Basel-Stadt, Switzerland (approval no. 2655).

Generation of GATA2VENUS Knockin Reporter Mouse Line

The GATA2VENUS knockin construct consists of a 5.0-kbps 5′ end homology arm lasting until the last codon of *Gata2* (skipping the endogenous stop-codon) followed by a short linker sequence, the coding sequence of *Venus*, FRT (Flp recognition target)-flanked neomycin resistance gene cassette, and a 5-kbps 3′ end homology arm. JM8.A3 ESCs (C57BL/6J background) were electroporated with the targeting vector and selected using 0.2 mg/mL G418 and 2 μM ganciclovir. Colonies were screened by Southern blot for correct integration events using 5′ and 3′ end external probes. Germline chimeras were generated from correct ESC clone by ESC aggregation. FRT-flanked neo-selection cassette was excised *in vivo* by crossing with an Flpe deleter strain (Dymecki, 1996). The resulting GATA2VENUS offspring were backcrossed for more than five generations with C57BL/6J animals.

Peripheral Blood Analysis

Male mice for peripheral blood analysis were euthanized, 0.5 mL blood was collected through cardiac puncture, and blood counts were analyzed using a VetABC Plus+ analyzer machine.

HSPC Analysis and Isolation

Analysis and isolation of primary HSPCs was performed according to previously described protocols (Arinobu et al., 2005; Cabezas-Wallscheid et al., 2014; Chen et al., 2005; Hettinger et al., 2013; Iwasaki et al., 2005; Kiel et al., 2005; Pop et al., 2010; Pronk et al., 2007; Qi et al., 2013; Wilson et al., 2008; Yanez et al., 2017) using BD FACSAria III (BD Biosciences).

Bulk- and Single-Cell HSPC Culture and Analysis

HSPC culture was performed in pan-myeloid conditions as described previously (Drissen et al., 2016). For bulk colony assays, 100–200 HSPCs were seeded in 24-well plates (Thermo Scientific) and resulting cultures after 8 days were analyzed either by morphology (May-Grünwald Giemsa staining) or flow cytometry of lineage-specific surface markers. For single-cell colony assays, HSPCs were single-cell sorted into plastic-bottom 384-well plates (Greiner Bio-One) using BD FACSAria III (BD Biosciences). Analyses of single-cell colony assays after 8 days were performed using live-in culture antibody staining (Eilken et al., 2011; Endele et al.,

2017; Hoppe et al., 2016; Loeffler et al., 2018) and fluorescence imaging using a Nikon Eclipse Ti-E microscope. Quantification of the number of cells per colony was performed using fastER (Hilsenbeck et al., 2017).

Immunostaining of TFs

Freshly sorted HSPCs were seeded in poly-L-lysine- (Sigma Aldrich)-coated 384-well plates (Greiner Bio-One) and immunostaining of TFs was performed according to protocols as described previously (Etzrodt et al., 2018; Hoppe et al., 2016) using the indicated antibodies (Table S5). Images were acquired using a Nikon Eclipse Ti-E microscope and quantification of TF intensities was performed using a BaSiC background analyzer (Peng et al., 2017) and fastER segmentation tool (Hilsenbeck et al., 2017). For *in situ* imaging of embryos, E14 embryos were frozen, embedded on PolyFreeze, sliced in a cryostat on glass slides, fixed with 4% paraformaldehyde for 20 min at room temperature, and immunostained using indicated antibodies. Sections were imaged on a Leica TCS SP5 confocal microscope. *In situ* immunostaining of GATA2 TF in kidney was performed according to protocols described previously (Coutu et al., 2017, 2018) and imaged on a Leica TCS SP8 confocal microscope.

Protein Stability Assay of TFs

HSPCs were cultured as described above and treated with 50 μM cycloheximide (Sigma Aldrich). Cells were fixed at the indicated time points using 4% paraformaldehyde (Sigma Aldrich) and subjected to the standard immunostaining protocol (as described above) (Hoppe et al., 2016).

Statistical Analyses

The error bars in this report indicate SDs. Sample means with SDs were derived from the indicated numbers of mice. Each mouse represents an independent replicate. The difference between two samples was analyzed by using either two-sample t test or two-sided Wilcoxon rank-sum test with continuity correction after normality analysis with custom written codes in R.

DATA AND CODE AVAILABILITY

Data is available upon request.

SUPPLEMENTAL INFORMATION

Supplemental Information can be found online at https://doi.org/10.1016/j.stemcr.2020.06.008.

AUTHOR CONTRIBUTIONS

N.A. planned and performed the experiments and analyzed data. P.S.H. cloned knockin constructs and provided technical support for TF immunostaining protocols with M.E. L.K. and G.C.O. performed *in situ* immunostaining of adult and embryonic tissues, respectively. D.L. supported the imaging. O.H. programmed the software. K.A. generated GATA2VENUS ESCs. T.S. designed and supervised the study, analyzed data, and wrote the manuscript with N.A. All authors read and commented on final manuscript.

ACKNOWLEDGMENTS

We are grateful to G. Camenisch and M. Hussherr of the D-BSSE mouse facility for animal handling, the EPIC facility of ETH Zurich for GATA2 mouse line generation from ESCs and the D-BSSE SCU for flow cytometry and imaging support. We thank P. Dettinger for reviewing the manuscript. This work was supported by Swiss National Science Foundation grant to T.S. and EMBO long-term fellowship to M.E. T.S. and O.H. acknowledge financial support from SystemsX.ch.

Received: January 13, 2020
Revised: June 8, 2020
Accepted: June 9, 2020
Published: July 09, 2020

REFERENCES

Akashi, K., Traver, D., Miyamoto, T., and Weissman, I.L. (2000). A clonogenic common myeloid progenitor that gives rise to all myeloid lineages. Nature *404*, 193–197.

Arinobu, Y., Iwasaki, H., Gurish, M.F., Mizuno, S., Shigematsu, H., Ozawa, H., Tenen, D.G., Austen, K.F., and Akashi, K. (2005). Developmental checkpoints of basophil/mast cell lineages in adult murine hematopoiesis. Proc. Natl. Acad. Sci. U S A *102*, 1–6.

Bresnick, E.H., Martowicz, M., Pal, S., and Johnson, K.D. (2005). Developmental control via GATA factor interplay at chromatin domains. J. Cell. Physiol. *205*, 1–9.

Bresnick, E.H., Lee, H.Y., Fujiwara, T., Johnson, K.D., and Keles, S. (2010). GATA switches as developmental drivers. J. Biol. Chem. *285*, 31087–31093.

Cabezas-Wallscheid, N., Klimmeck, D., Hansson, J., Lipka, D.B., Reyes, A., Wang, Q., Weichenhan, D., Lier, A., Von Paleske, L., Renders, S., et al. (2014). Identification of regulatory networks in HSCs and their immediate progeny via integrated proteome, transcriptome, and DNA methylome analysis. Cell Stem Cell *15*, 507–522.

Cantor, A.B., Iwasaki, H., Arinobu, Y., Moran, T.B., Shigematsu, H., Sullivan, M.R., Akashi, K., and Orkin, S.H. (2008). Antagonism of FOG-1 and GATA factors in fate choice for the mast cell lineage. J. Exp. Med. *205*, 611–624.

Charles, M.A., Saunde, T.L., Wood, W.M., Owens, K., Parlow, A.F., Camper, S.A., Ridgway, E.C., and Gordon, D.F. (2006). Pituitary-specific Gata2 knockout: effects on gonadotrope and thyrotrope function. Mol. Endocrinol. *20*, 1366–1377.

Chen, C.-C., Grimbaldeston, M.A., Tsai, M., Weissman, I.L., and Galli, S.J. (2005). Identification of mast cell progenitors in adult mice. Proc. Natl. Acad. Sci. U S A *102*, 11408–11413.

Coutu, D.L., Kokkaliaris, K.D., Kunz, L., and Schroeder, T. (2017). Three-dimensional map of nonhematopoietic bone and bone-marrow cells and molecules. Nat. Biotechnol. *35*, 1202–1210.

Coutu, D.L., Kokkaliaris, K.D., Kunz, L., and Schroeder, T. (2018). Multicolor quantitative confocal imaging cytometry. Nat. Methods *15*, 39–46.

Dahlin, J.S., Hamey, F.K., Pijuan-Sala, B., Shepherd, M., Lau, W.W.Y., Nestorowa, S., Weinreb, C., Wolock, S., Hannah, R., Diamanti, E., et al. (2018). A single-cell hematopoietic landscape

resolves 8 lineage trajectories and defects in Kit mutant mice. Blood *131*, e1–e11.

Dasen, J.S., O'Connell, S.M., Flynn, S.E., Treier, M., Gleiberman, A.S., Szeto, D.P., Hooshmand, F., Aggarwal, A.K., and Rosenfeld, M.G. (1999). Reciprocal interactions of Pit1 and GATA2 mediate signaling gradient- induced determination of pituitary cell types. Cell *97*, 587–598.

Doré, L.C., Chlon, T.M., Brown, C.D., White, K.P., and Crispino, J.D. (2012). Chromatin occupancy analysis reveals genome-wide GATA factor switching during hematopoiesis. Blood *119*, 3724–3733.

Drissen, R., Buza-Vidas, N., Woll, P., Thongjuea, S., Gambardella, A., Giustacchini, A., Mancini, E., Zriwil, A., Lutteropp, M., Grover, A., et al. (2016). Distinct myeloid progenitor-differentiation pathways identified through single-cell RNA sequencing. Nat. Immunol. *17*, 666–676.

Dymecki, S.M. (1996). Flp recombinase promotes site-specific DNA recombination in embryonic stem cells and transgenic mice. Proc. Natl. Acad. Sci. U S A *93*, 6191–6196.

Eich, C., Arlt, J., Vink, C.S., Solaimani Kartalaei, P., Kaimakis, P., Mariani, S.A., van der Linden, R., van Cappellen, W.A., and Dzierzak, E. (2018). In vivo single cell analysis reveals Gata2 dynamics in cells transitioning to hematopoietic fate. J. Exp. Med. *215*, 233–248.

Eilken, H., Rieger, M., Hoppe, P., Hermann, A., Smejkal, B., Drew, E., Thum, M., Ninkovic, J., and Beckervordersandforth, R. (2011). Continuous long-term detection of live cell surface markers by 'in culture' antibody staining. Protocol Exchange https://doi.org/10.1038/protex.2011.205.

Eilken, H.M., Nishikawa, S.I., and Schroeder, T. (2009). Continuous single-cell imaging of blood generation from haemogenic endothelium. Nature *457*, 896–900.

Endele, M., Loeffler, D., Kokkaliaris, K.D., Hilsenbeck, O., Skylaki, S., Hoppe, P.S., Schambach, A., Stanley, E.R., and Schroeder, T. (2017). CSF-1-induced Src signaling can instruct monocytic lineage choice. Blood *129*, 1691–1701.

Etzrodt, M., and Schroeder, T. (2017). Illuminating stem cell transcription factor dynamics: long-term single-cell imaging of fluorescent protein fusions. Curr. Opin. Cell Biol. *49*, 77–83.

Etzrodt, M., Endele, M., and Schroeder, T. (2014). Quantitative single-cell approaches to stem cell research. Cell Stem Cell *15*, 546–558.

Etzrodt, M., Ahmed, N., Hoppe, P.S., Loeffler, D., Skylaki, S., Hilsenbeck, O., Kokkaliaris, K.D., Kaltenbach, H.-M., Stelling, J., Nerlov, C., et al. (2018). Inflammatory signals directly instruct PU.1 in HSCs via TNF. Blood *133*, 816–819.

Filipczyk, A., Marr, C., Hastreiter, S., Feigelman, J., Schwarzfischer, M., Hoppe, P.S., Loeffler, D., Kokkaliaris, K.D., Endele, M., Schauberger, B., et al. (2015). Network plasticity of pluripotency transcription factors in embryonic stem cells. Nat. Cell Biol. *17*, 1235–1246.

Gao, X., Johnson, K.D., Chang, Y.-I., Boyer, M.E., Dewey, C.N., Zhang, J., and Bresnick, E.H. (2013). *Gata2* cis-element is required for hematopoietic stem cell generation in the mammalian embryo. J. Exp. Med. *210*, 2833–2842.

Graf, T., and Enver, T. (2009). Forcing cells to change lineages. Nature *462*, 587–594.

Grass, J.A., Boyer, M.E., Pal, S., Wu, J., Weiss, M.J., and Bresnick, E.H. (2003). GATA-1-dependent transcriptional repression of GATA-2 via disruption of positive autoregulation and domain-wide chromatin remodeling. Proc. Natl. Acad. Sci. U S A *100*, 8811–8816.

Hettinger, J., Richards, D.M., Hansson, J., Barra, M.M., Joschko, A.C., Krijgsveld, J., and Feuerer, M. (2013). Origin of monocytes and macrophages in a committed progenitor. Nat. Immunol. *14*, 821–830.

Hilsenbeck, O., Schwarzfischer, M., Loeffler, Di., DImopoulos, S., Hastreiter, S., Marr, C., Theis, F.J., and Schroeder, T. (2017). FastER: a user-friendly tool for ultrafast and robust cell segmentation in large-scale microscopy. Bioinformatics *33*, 2020–2028.

Hoppe, P.S., Coutu, D.L., and Schroeder, T. (2014). Single-cell technologies sharpen up mammalian stem cell research. Nat. Cell Biol. *16*, 919–927.

Hoppe, P.S., Schwarzfischer, M., Loeffler, D., Kokkaliaris, K.D., Hilsenbeck, O., Moritz, N., Endele, M., Filipczyk, A., Gambardella, A., Ahmed, N., et al. (2016). Early myeloid lineage choice is not initiated by random PU.1 to GATA1 protein ratios. Nature *535*, 299–302.

Iwasaki, H., Mizuno, S., Mayfield, R., Shigematsu, H., Arinobu, Y., Seed, B., Gurish, M.F., Takatsu, K., and Akashi, K. (2005). Identification of eosinophil lineage-committed progenitors in the murine bone marrow. J. Exp. Med. *201*, 1891–1897.

Iwasaki, H., Mizuno, S.I., Arinobu, Y., Ozawa, H., Mori, Y., Shigematsu, H., Takatsu, K., Tenen, D.G., and Akashi, K. (2006). The order of expression of transcription factors directs hierarchical specification of hematopoietic lineages. Genes Dev. *20*, 3010–3021.

Kaimakis, P., De Pater, E., Eich, C., Kartalaei, P.S., Kauts, M., Vink, C.S., Van Der Linden, R., Jaegle, M., Yokomizo, T., Meijer, D., et al. (2016). Functional and molecular characterization of mouse Gata2-independent hematopoietic progenitors (blood-2015-10-673749.full). Blood *127*, 1426–1438.

Kauts, M.L., De Leo, B., Rodríguez-Seoane, C., Ronn, R., Glykofrydis, F., Maglitto, A., Kaimakis, P., Basi, M., Taylor, H., Forrester, L., et al. (2018). Rapid mast cell generation from Gata2 reporter pluripotent stem cells. Stem Cell Reports *11*, 1009–1020.

Khandekar, M., Suzuki, N., Lewton, J., Yamamoto, M., and Douglas Engel, J. (2004). Multiple, distant Gata2 enhancers specify temporally and tissue-specific patterning in the developing urogenital system. Mol. Cell. Biol. *24*, 10263–10276.

Kiel, M.J., Yilmaz, O.H., Iwashita, T., Yilmaz, O.H., Terhorst, C., and Morrison, S.J. (2005). SLAM family receptors distinguish hematopoietic stem and progenitor cells and reveal endothelial niches for stem cells. Cell *121*, 1109–1121.

Krumsiek, J., Marr, C., Schroeder, T., and Theis, F.J. (2011). Hierarchical differentiation of myeloid progenitors is encoded in the transcription factor network. PLoS One *6*, e22649.

Kueh, H.Y., Champhekhar, A., Nutt, S.L., Elowitz, M.B., and Rothenberg, E.V. (2013). Positive feedback between PU.1 and the cell cycle controls myeloid differentiation. Science *341*, 670–673.

Lee, T.I., and Young, R.A. (2013). Transcriptional regulation and its misregulation in disease. Cell *152*, 1237–1251.

Li, Y., Qi, X., Liu, B., and Huang, H. (2015). The STAT5–GATA2 pathway is critical in basophil and mast cell differentiation and maintenance. J. Immunol. *194*, 4328–4338.

Ling, K.-W., Ottersbach, K., van Hamburg, J.P., Oziemlak, A., Tsai, F.-Y., Orkin, S.H., Ploemacher, R., Hendriks, R.W., and Dzierzak, E. (2004). GATA-2 plays two functionally distinct roles during the ontogeny of hematopoietic stem cells. J. Exp. Med. *200*, 871–882.

Loeffler, D., and Schroeder, T. (2019). Understanding cell fate control by continuous single cell quantification. Blood *133*, 1406–1414.

Loeffler, D., Wang, W., Hopf, A., Hilsenbeck, O., Bourgine, P.E., Rudolf, F., Martin, I., and Schroeder, T. (2018). Mouse and human HSPC immobilization in liquid culture by CD43- or CD44-antibody coating. Blood *131*, 1425–1429.

McGrath, K.E., Frame, J.M., Fegan, K.H., Bowen, J.R., Conway, S.J., Catherman, S.C., Kingsley, P.D., Koniski, A.D., and Palis, J. (2015). Distinct sources of hematopoietic progenitors emerge before HSCs and provide functional blood cells in the mammalian embryo. Cell Rep. *11*, 1892–1904.

McIvor, Z., Hein, S., Fiegler, H., Schroeder, T., Stocking, C., Just, U., and Cross, M. (2003). Transient expression of PU.1 commits multipotent progenitors to a myeloid fate whereas continued expression favors macrophage over granulocyte differentiation. Exp. Hematol. *31*, 39–47.

Minami, T., Murakami, T., Horiuchi, K., Miura, M., Noguchi, T., Miyazaki, J.I., Hamakubo, T., Aird, W.C., and Kodama, T. (2004). Interaction between Hex and GATA transcription factors in vascular endothelial cells inhibits flk-1/KDR-mediated vascular endothelial growth factor signaling. J. Biol. Chem. *279*, 20626–20635.

Nagai, T., Ibata, K., Park, E.S., Kubota, M., and Mikoshiba, K. (2002). A variant of yellow fluorescent protein with fast and efficient maturation for cell-biological applications. Nat. Biotechnol. *20*, 87–90.

Nardelli, J., Thiesson, D., Fujiwara, Y., Tsai, F.Y., and Orkin, S.H. (1999). Expression and genetic interaction of transcription factors GATA-2 and GATA-3 during development of the mouse central nervous system. Dev. Biol. *210*, 305–321.

Ohmori, S., Takai, J., Ishijima, Y., Suzuki, M., Moriguchi, T., Philipsen, S., Yamamoto, M., and Ohneda, K. (2012). Regulation of GATA factor expression is distinct between erythroid and mast cell lineages. Mol. Cell. Biol. *32*, 4742–4755.

Ohmori, S.N.Y., Moriguchi, T., Noguchi, Y., Ikeda, M., Kobayashi, K., Tomaru, N., Ishijima, Y., Ohneda, O., Yamamoto, M., and Ohneda, K. (2015). GATA2 is critical for the maintenance of cellular identity in differentiated mast cells derived from mouse bone marrow. Blood *125*, 3306–3315.

Okita, C., Sato, M., and Schroeder, T. (2004). Generation of optimized yellow and red fluorescent proteins with distinct subcellular localization. Biotechniques *36*, 418–424.

de Pater, E., Kaimakis, P., Vink, C.S., Yokomizo, T., Yamada-Inagawa, T., van der Linden, R., Kartalaei, P.S., Camper, S.A., Speck, N., and Dzierzak, E. (2013). *Gata2* is required for HSC generation and survival. J. Exp. Med. *210*, 2843–2850.

Peng, T., Thorn, K., Schroeder, T., Wang, L., Theis, F.J., Marr, C., and Navab, N. (2017). A BaSiC tool for background and shading correction of optical microscopy images. Nat. Commun. *8*, 1–7.

Persons, B.D.A., Allay, J.A., Allay, E.R., Ashmun, R.A., Orlic, D., Jane, S.M., Cunningham, J.M., and Nienhuis, A.W. (1999). Enforced expression of the GATA-2 transcription factor blocks normal hematopoiesis. In Vitro *93*, 488–499.

Pietras, E.M., Reynaud, D., Kang, Y.-A., Carlin, D., Calero-Nieto, F.J., Leavitt, A.D., Stuart, J.M., Gottgens, B., and Passegué, E. (2015). Functionally distinct subsets of lineage-biased multipotent progenitors control blood production in normal and regenerative conditions. Cell Stem Cell *17*, 35–46.

Pop, R., Shearstone, J.R., Shen, Q., Liu, Y., Hallstrom, K., Koulnis, M., Gribnau, J., and Socolovsky, M. (2010). A key commitment step in erythropoiesis is synchronized with the cell cycle clock through mutual inhibition between PU.1 and S-phase progression. PLoS Biol. *8*, e1000484.

Pronk, C.J.H., Rossi, D.J., Månsson, R., Attema, J.L., Norddahl, G.L., Chan, C.K.F., Sigvardsson, M., Weissman, I.L., and Bryder, D. (2007). Elucidation of the phenotypic, functional, and molecular topography of a myeloerythroid progenitor cell hierarchy. Cell Stem Cell *1*, 428–442.

Qi, X., Hong, J., Chaves, L., Zhuang, Y., Chen, Y., Wang, D., Chabon, J., Graham, B., Ohmori, K., Li, Y., et al. (2013). Antagonistic regulation by the transcription factors C/EBPα and MITF specifies basophil and mast cell fates. Immunity *39*, 97–110.

Ray, S., Dutta, D., Karim Rumi, M.A., Kent, L.N., Soares, M.J., and Paul, S. (2009). Context-dependent function of regulatory elements and a switch in chromatin occupancy between GATA3 and GATA2 regulate Gata2 transcription during trophoblast differentiation. J. Biol. Chem. *284*, 4978–4988.

Rodrigues, N.P., Janzen, V., Forkert, R., Dombkowski, D.M., Boyd, A.S., Orkin, S.H., Enver, T., Vyas, P., and Scadden, D.T. (2005). Haploinsufficiency of GATA-2 perturbs adult hematopoietic stem-cell homeostasis. Blood *106*, 477–484.

Schroeder, T. (2005). Tracking hematopoiesis at the single cell level. Ann. N. Y. Acad. Sci. *1044*, 201–209.

Shimizu, R., and Yamamoto, M. (2005). Gene expression regulation and domain function of hematopoietic GATA factors. Semin. Cell Dev. Biol. *16*, 129–136.

Siggers, P., Smith, L., and Greenfield, A. (2002). Sexually dimorphic expression of Gata-2 during mouse gonad development. Mech. Dev. *111*, 159–162.

Snow, J.W., Trowbridge, J.J., Johnson, K.D., Fujiwara, T., Emambokus, N.E., Grass, J.A., Orkin, S.H., Bresnick, E.H., and Dc, W. (2011). Context-dependent function of "GATA switch" sites in vivo. Blood *117*, 4769–4772.

Spitz, F., and Furlong, E.E.M. (2012). Transcription factors: from enhancer binding to developmental control. Nat. Rev. Genet. *13*, 613–626.

Suzuki, N., Ohneda, O., Minegishi, N., Nishikawa, M., Ohta, T., Takahashi, S., Engel, J.D., and Yamamoto, M. (2006). Combinatorial

Gata2 and Sca1 expression defines hematopoietic stem cells in the bone marrow niche. Proc. Natl. Acad. Sci. U S A *103*, 2202–2207.

Tong, Q., Dalgin, G., Xu, H., Ting, C.N., Leiden, J.M., and Hotamisligil, G.S. (2000). Function of GATA transcription factors in preadipocyte-adipocyte transition. Science *290*, 134–138.

Tong, Q., Tsai, J., Tan, G., Dalgin, G., and Hotamisligil, G.S. (2005). Interaction between GATA and the C/EBP family of transcription factors is critical in GATA-mediated suppression of adipocyte differentiation. Mol. Cell. Biol. *2*, 706–715.

Tsai, F.-Y., Keller, G., Kuo, F.C., Weiss, M., Chen, J., Rosenblatt, M., Alt, F.W., and Orkin, S.H. (1994). An early hematopoietic defect in mice lacking the transcription factor GATA-2. Nature *371*, 221–226.

Walsh, J.C., DeKoter, R.P., Lee, H.J., Smith, E.D., Lancki, D.W., Gurish, M.F., Friend, D.S., Stevens, R.L., Anastasi, J., and Singh, H. (2002). Cooperative and antagonistic interplay between PU.1 and GATA-2 in the specification of myeloid cell fates. Immunity *17*, 665–676.

Weinreb, C., Rodriguez-Fraticelli, A., Camargo, F.D., and Klein, A.M. (2020). Lineage tracing on transcriptional landscapes links state to fate during differentiation Caleb. Science *367*, eaaw3381.

Wilson, A., Laurenti, E., Oser, G., van der Wath, R.C., Blanco-Bose, W., Jaworski, M., Offner, S., Dunant, C.F., Eshkind, L., Bockamp, E., et al. (2008). Hematopoietic stem cells reversibly switch from dormancy to self-renewal during homeostasis and repair. Cell *135*, 1118–1129.

Yanez, A., Ng, M.Y., Hassanzadeh-kiabi, N., and Goodridge, H.S. (2017). IRF8 acts in lineage-committed rather than oligopotent progenitors to control neutrophil vs monocyte production. Comparative Study *125*, 1452–1460.

Zhou, Y. (1998). Rescue of the embryonic lethal hematopoietic defect reveals a critical role for GATA-2 in urogenital development. EMBO J. *17*, 6689–6700.

Stem Cell Reports, Volume *15*

Supplemental Information

A Novel GATA2 Protein Reporter Mouse Reveals Hematopoietic Progenitor Cell Types

Nouraiz Ahmed, Leo Kunz, Philipp S. Hoppe, Dirk Loeffler, Martin Etzrodt, Germán Camargo Ortega, Oliver Hilsenbeck, Konstantinos Anastassiadis, and Timm Schroeder

Supplemental information:

Supplemental Figures:

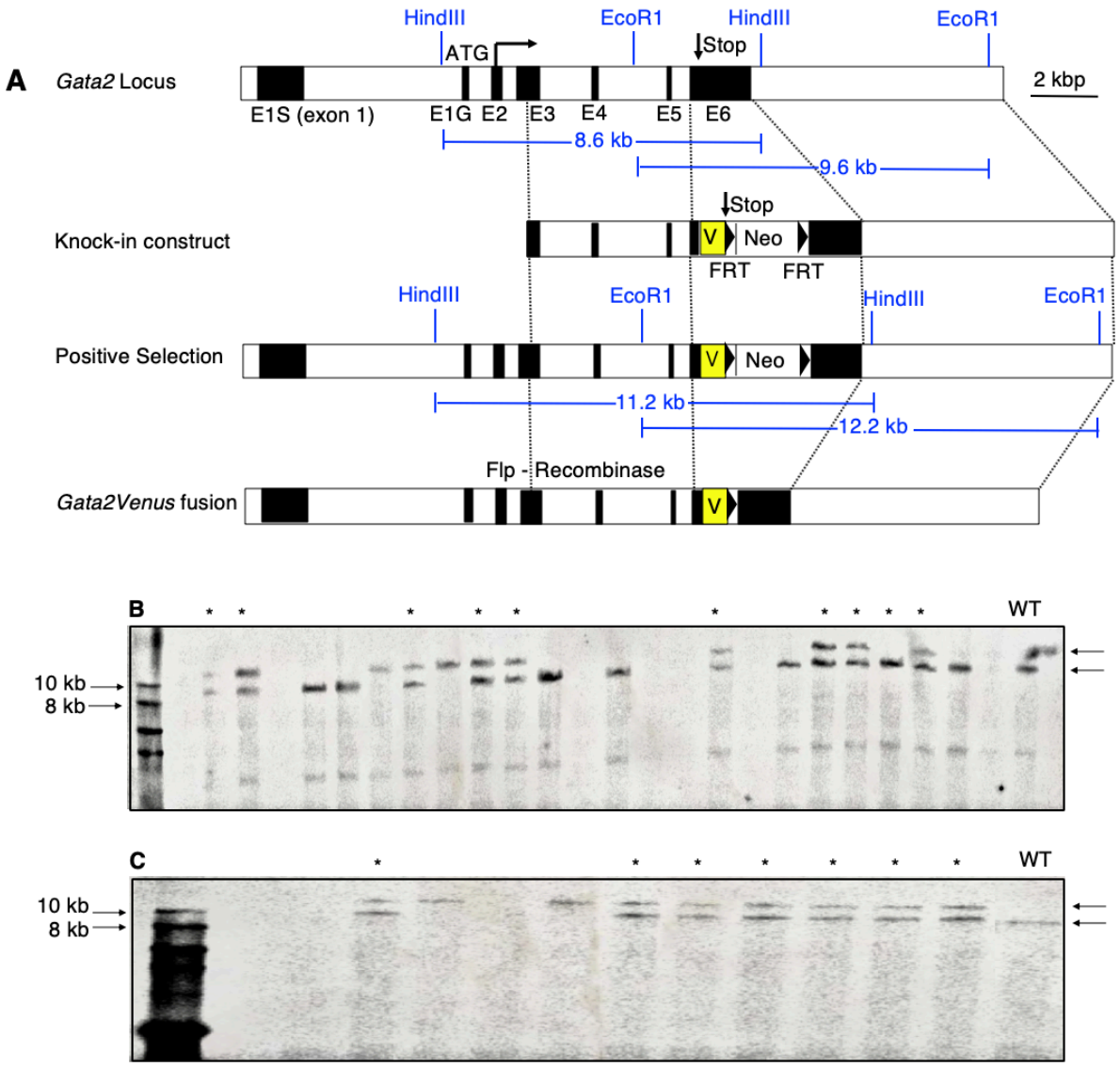

Figure S1. Correct integration of *Gata2Venus* cassette (see main figure 1). (A) Schematic illustration of generation of *Gata2* allele with *Venus* fusion before STOP codon in Exon VI. Restriction sites and expected band size for 5′ and 3′ southern blot probes are shown in blue. **(B)** 5′ end southern blot image to show correct integration of *Gata2Venus* cassette in mouse genome. The genomic DNA was digested with HindIII and hybridized with a 5′ probe. Correct 5′ end integration was confirmed in 10 ESC clones (indicated with stars). Top band (11261 bp) indicates knock-in allele and bottom band (8643 bp) indicates wild-type allele. **(C)** 3′ end southern blot image to highlight correct integration of *Gata2Venus* cassette in mouse genome. The genomic DNA was digested with EcoRI and hybridized with a 3′ probe (grey bar). 7 out of 10 clones exhibited correct 3′ integration (indicated with stars). Top band (12286 bp) indicates knock-in allele and bottom band (9671 bp) indicates wild-type allele. Arrows in **B** and **C** indicate position of DNA marker (left) and genomic DNA bands (right). (see main figure 1)

Type of cross	Pups born	Expected genotype frequency			Observed genotype frequency		
		homo	het	wt	homo	het	wt
homo X wt	24	0	1	0	0	1	0
het X wt	29	0	0.5	0.5	0	0.45	0.55
het X het	22	0.25	0.5	0.25	0.27	0.5	0.23
homo X het	26	0.5	0.5	0	0.5	0.5	0
homo X homo	41	1	0	0	1	0	0

Figure S2. Mendelian frequency is not altered in GATA2VENUS mouse line (see main figure 1). Mice with different genotype backgrounds of GATA2VENUS allele were crossed and resulting frequency of offspring genotypes was quantified and compared to expected frequency for > 6 litters born. Different types of crosses include (1) GATA2VENUS homozygous (homo) crossed with wild-type (wt), (2) GATA2VENUS heterozygous (het) crossed with wild-type (wt), (3) GATA2VENUS heterozygous (het) crossed with GATA2VENUS heterozygous (het), (4) GATA2VENUS homozygous (homo) crossed with GATA2VENUS heterozygous (het) and (5) GATA2VENUS homozygous (homo) crossed with GATA2VENUS homozygous (homo) mice. (see main figure 1)

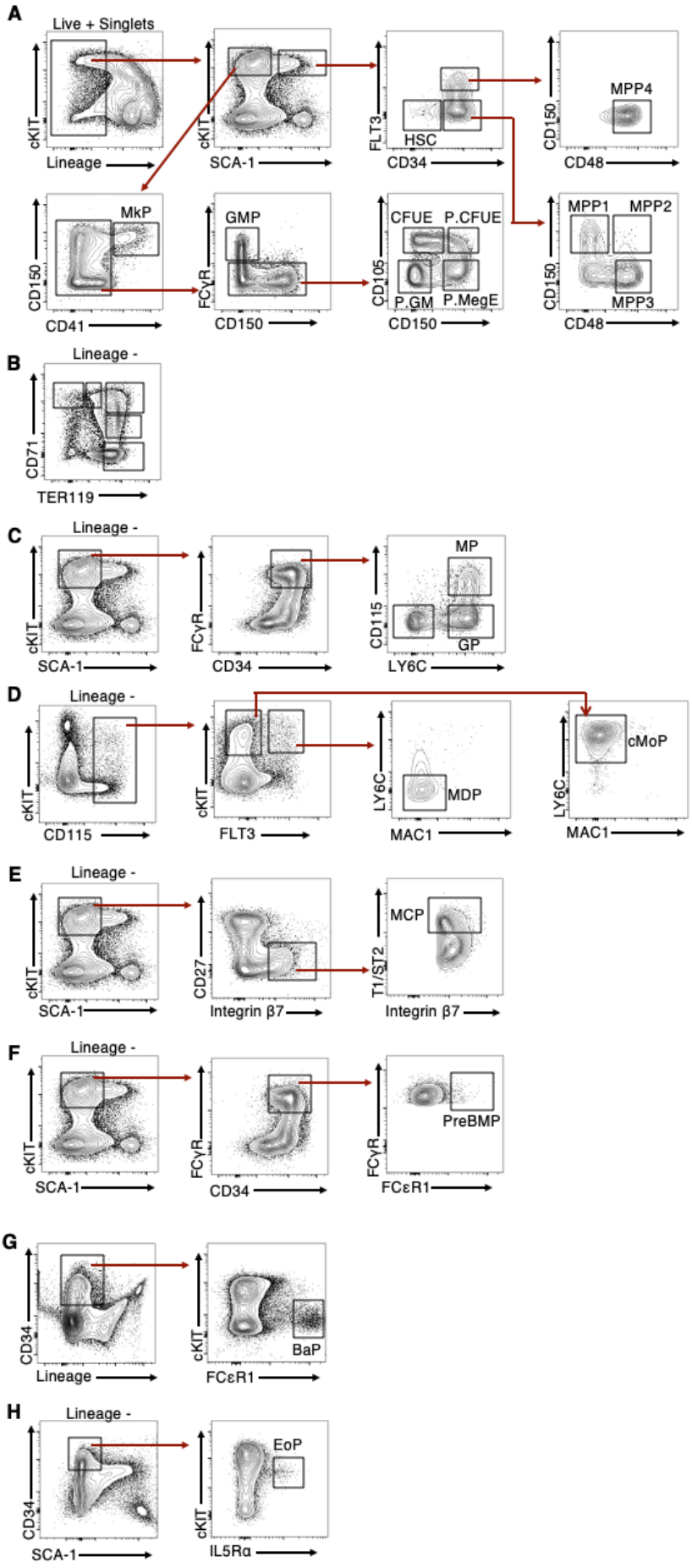

Figure S3. FACS gating scheme used for analysis and isolation of hematopoietic stem and progenitor cells (see main figure 3).
(A) HSC – Hematopoietic Stem Cell, MPP 1-4 – Multipotent Progenitor 1-4, P.MegE – pre Megakaryocyte Erythrocyte, MkP – Megakaryocyte progenitor, P.CFUE – pre colony forming unit Erythrocyte, CFUE – colony forming unit Erythrocyte, preGM – pre Granulocyte Monocyte, GMP – Granulocyte Monocyte Progenitor. **(B)** Erythrocyte differentiation stages based on CD71 and TER119 expression. **(C)** MP – Monocyte progenitor, GP – Granulocyte progenitor. **(D)** MDP – Monocyte Dendritic cell progenitor, cMoP – common Monocyte progenitor. **(E)** MCP – Mast cell progenitor. **(F)** preBMP – pre Basophil Mast cell progenitor. **(G)** BaP – Basophil progenitor. **(H)** EoP – Eosinophil progenitor. (see main figure 3)

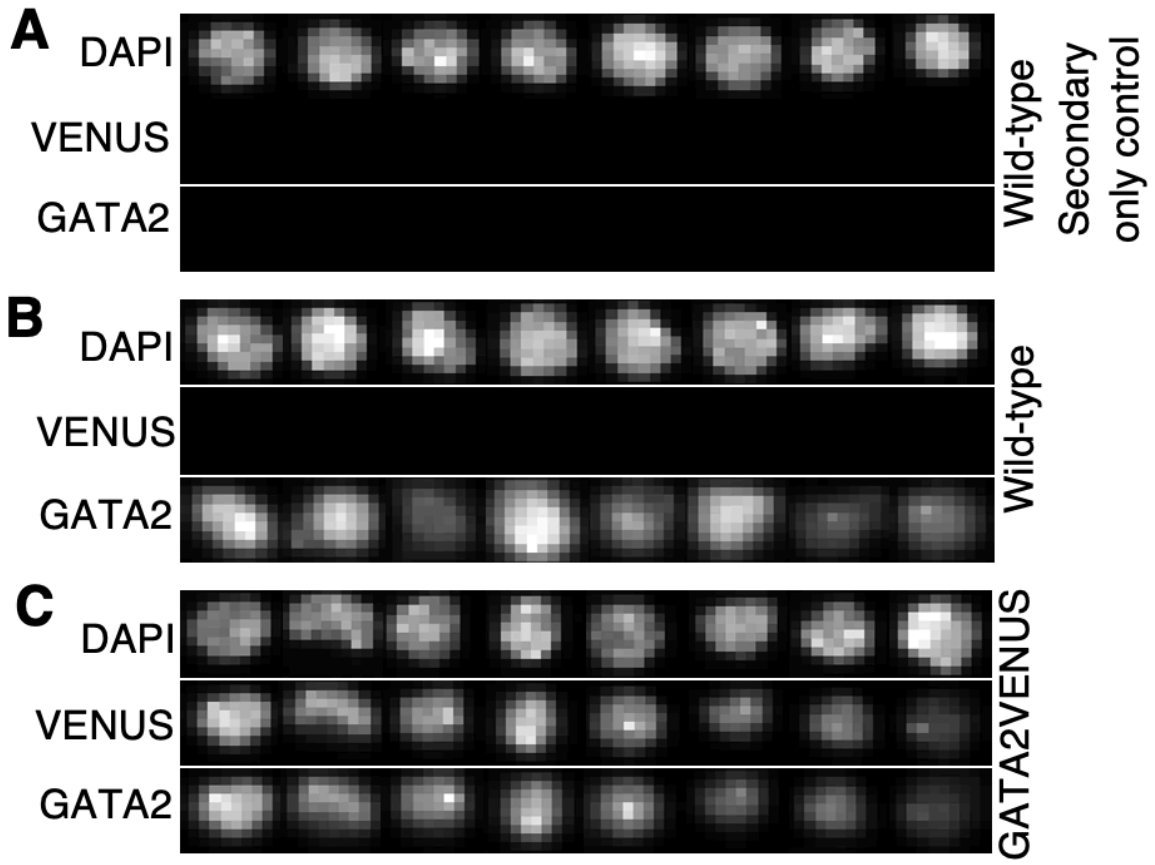

Supplementary Figure S4. Colocalization of GATA2 and VENUS signal inside GATA2VENUS nuclei (see main figure 1). Localization of GATA2 and VENUS in P.MegE from wild-type mouse (VENUS negative control) without **(A)** and with **(B)** primary anti-GATA2 antibody. **(C)** With primary anti-GATA2 antibody in GATA2VENUS P.MegE. See Figure 1K. Image tile: 10 µm.

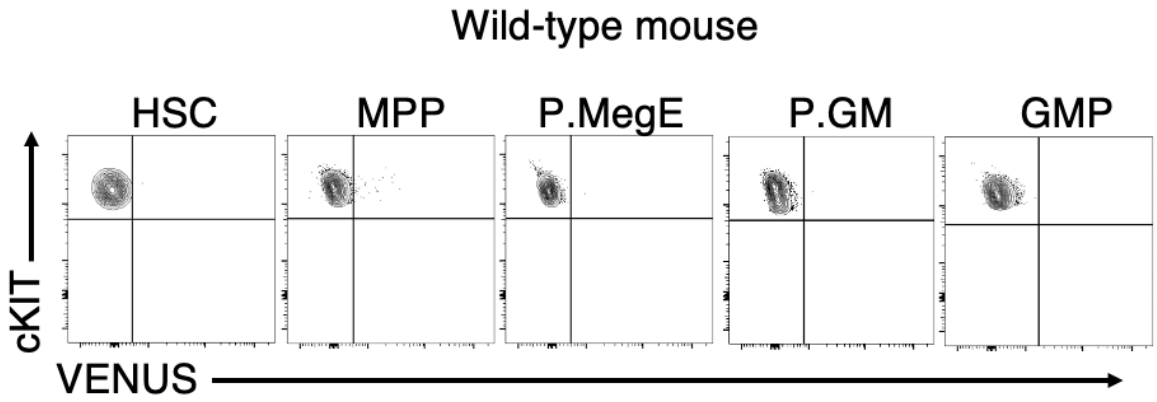

Figure S5. VENUS fluorescence channel background in wild-type HSPCs (see main figure 3). FACS of VENUS channel in HSPCs from a 12-week old wild-type mouse. Used to set background levels of GATA2VENUS expression in cells from GATA2VENUS mouse line in Figure 3.
Abbreviations: HSC – Hematopoietic Stem Cell, MPP – Multipotent Progenitor, P.MegE – pre Megakaryocyte Erythrocyte, preGM – pre Granulocyte Monocyte, GMP – Granulocyte Monocyte Progenitor. (see main figure 3)

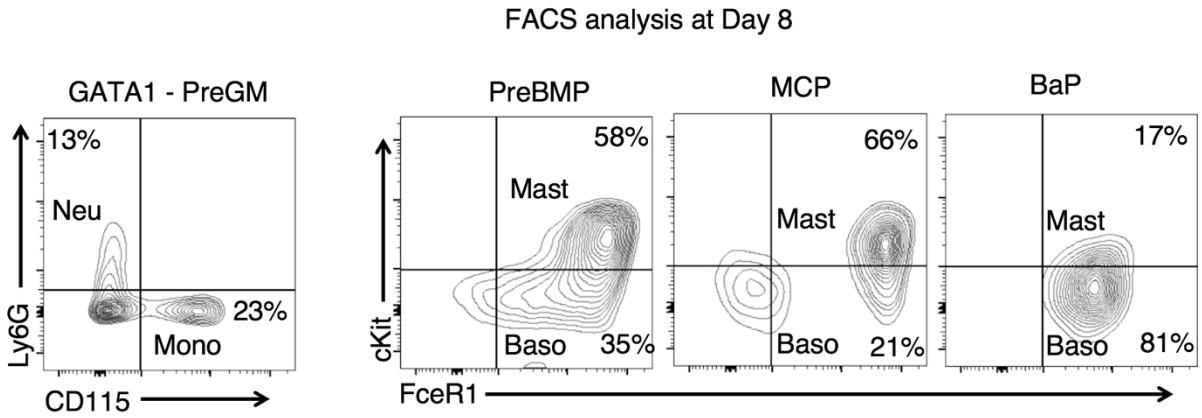

Figure S6. Pan myeloid media conditions support survival, proliferation and differentiation of different granulocyte and monocyte lineages (see main figure 5 & 6). GATA1-low preGMs, preBMPs, MCPs and BaPs from PU.1eYFP/GATA1mCHERRY mice(Hoppe et al., 2016) were sorted and cultured for 8 days in pan myeloid media supporting survival, proliferation and differentiation of monocytes, neutrophils, basophils and mast cells. Mature cell types were detected at day 8 by flow cytometry analysis of lineage specific markers including $cKIT^{+}$ $FC\varepsilon R1^{+}$ cells (mast cells), $cKIT^{-}$ $FC\varepsilon R1^{+}$ cells (basophils), $LY6G^{+}$ cells (neutrophils) and $CD115^{+}$ cells (monocytes). Positive gates were set using unstained control cells.
Abbreviations: preGM – pre Granulocyte Monocyte, preBMP – pre Basophil Mast cell progenitor, MCP – Mast cell progenitor and BaP – Basophil progenitor. (see main figure 5 & 6)

Table S1: FACS gating scheme used for analysis and isolation of hematopoietic stem and progenitor cells. (Related to main figure 3)

Cell type	Surface marker combination	Ref
Lineage*	CD3e B220 CD19 CD11b Gr-1 TER119	(Cabezas-Wallscheid et al., 2014; Kiel et al., 2005; Wilson et al., 2008)
HSC	Lin$^-$ SCA-1$^+$ cKIT$^+$ CD135$^-$ CD34$^-$ CD48$^-$ CD150$^+$	(Cabezas-Wallscheid et al., 2014; Kiel et al., 2005; Wilson et al., 2008)
MPP1	Lin$^-$ SCA-1$^+$ cKIT$^+$ CD135$^-$ CD34$^+$ CD48$^-$ CD150$^+$	(Cabezas-Wallscheid et al., 2014; Kiel et al., 2005; Wilson et al., 2008)
MPP2	Lin$^-$ SCA-1$^+$ cKIT$^+$ CD135$^-$ CD34$^+$ CD48$^+$ CD150$^+$	(Cabezas-Wallscheid et al., 2014; Kiel et al., 2005; Wilson et al., 2008)
MPP3	Lin$^-$ SCA-1$^+$ cKIT$^+$ CD135$^-$ CD34$^+$ CD48$^+$ CD150$^-$	(Cabezas-Wallscheid et al., 2014; Kiel et al., 2005; Wilson et al., 2008)
MPP4	Lin$^-$ SCA-1$^+$ cKIT$^+$ CD135$^+$ CD34$^+$ CD48$^+$ CD150$^-$	(Cabezas-Wallscheid et al., 2014; Kiel et al., 2005; Wilson et al., 2008)
P. MegE	Lin$^-$ SCA-1$^-$ cKIT$^+$ CD16/32$^-$ CD41$^-$ CD105$^-$ CD150$^+$	(Pronk et al., 2007)
MkP	Lin$^-$ SCA1-$^-$ cKIT$^+$ CD16/32$^-$ CD41$^+$ CD105$^-$ CD150$^+$	(Pronk et al., 2007)
P. CFUE	Lin$^-$ SCA-1$^-$ cKIT$^+$ CD16/32$^-$ CD41$^-$ CD105$^+$ CD150$^+$	(Pronk et al., 2007)
CFUE	Lin$^-$ SCA-1$^-$ cKIT$^+$ CD16/32$^-$ CD41$^-$ CD105$^+$ CD150-	(Pronk et al., 2007)
Ery-S1	Lin- CD71^{high} TER119^{low}	(Pop et al., 2010)
Ery-S2	Lin- CD71^{high} TER119^{mid}	(Pop et al., 2010)
Ery-S3	Lin- CD71^{high} TER119^{high}	(Pop et al., 2010)
Ery-S4	Lin- CD71^{mid} TER119^{high}	(Pop et al., 2010)
Ery-S5	Lin- CD71^{low} TER119^{high}	(Pop et al., 2010)
preGM	Lin$^-$ SCA-1$^-$ cKIT$^+$ CD16/32$^-$ CD41$^-$ CD105$^-$ CD150$^-$	(Pronk et al., 2007)
GMP	Lin$^-$ SCA-1$^-$ cKIT$^+$ CD16/32$^+$ CD41$^-$ CD105$^-$ CD150$^-$	(Pronk et al., 2007)
MP	Lin$^-$ SCA-1$^-$ cKIT$^+$ CD16/32$^+$ CD34$^+$ Ly6C$^+$ CD115$^+$	(Yanez et al., 2017)
GP	Lin$^-$ SCA-1$^-$ cKIT$^+$ CD16/32$^+$ CD34$^+$ Ly6C$^+$ CD115$^-$	(Yanez et al., 2017)
cMoP	Lin$^-$ cKIT$^+$ CD115$^+$ CD135$^-$ LY6C$^+$ CD11b$^-$	(Hettinger et al., 2013)
MDP	Lin$^-$ cKIT$^+$ CD115$^+$ CD135$^+$ LY6C$^-$ CD11b$^-$	(Hettinger et al., 2013)
EoP	Lin$^-$ SCA-1$^-$ cKIT^{mid} CD34$^+$ IL5Rα$^+$	(Iwasaki et al., 2005)
preBMP	Lin$^-$ SCA-1$^-$ cKIT$^+$ CD16/32$^+$ CD34$^+$ FCεR1$^+$	(Qi et al., 2013)
BaP	Lin$^-$ cKIT$^-$ CD34$^+$ FCεR1$^+$	(Arinobu et al., 2005)
MCP	Lin$^-$ SCA-1$^-$ cKIT$^+$ CD27$^-$ Integrin β7$^+$ T1/ST2$^+$	(Chen et al., 2005)

*TER119 lineage antibody was omitted during analysis of Erythroid stages S1 – S5.
*CD11b lineage antibody was omitted during analysis of Eosinophil progenitors (EoPs) and Basophil progenitors (BaPs).

Table S2: List of antibodies for FACS analysis and isolation of HSPCs. (Related to experimental procedures)

Antigen	**Conjugation**	**Clone**	**Company**	**Catalog no**
Strepavidin (Lineage)	BV711	N/A	BD Biosciences	563262
SCA-1	Pacific blue PerCP-CY5.5	D7 D7	Biolegend eBiosciences	108120 45-5981-82
cKIT	PE-CY7 BV510	2B8 ACK2	eBiosciences Biolegend	25-1171-82 135119
CD135	PerCPeFL710 PECF594	A2F10 A2F10.1	eBioscience BD Bioscience	46-1351-82 562537
CD34	eFL660 eFL450	RAM34 RAM34	eBioscience eBioscience	50-0341-82 48-0341-82
CD48	APCeFL780	HM48-1	eBioscience	47-0481-82
CD150	PE	TC15-12F12.2	Biolegend	115904
CD16/32	PE-CY7 APC-CY7	93 93	Biolegend Biolegend	101317 101328
CD41	BV605	MWReg30	BD Biosciences	563317
CD105	APC	MJ7/18	Biolegend	120414
CD71	APC	R17.217.1.4	eBioscience	17-0711-82
TER119	APCeFL780	Ter-119	eBioscience	47-5921-82
T1/ST2	PE	DIH9	Biolegend	145304
IL5Ra	PE	DIH37	Biolegend	153404
CD115	PE	AFS98	eBioscience	12-1152-82
Integrin B7	PE-CY7	FIB504	eBioscience	25-5867-41
FCeR1	APC	MAR-1	eBioscience	17-5898-82
CD11b	APC	M1/70	eBioscience	17-0112-81
CD27	APC-CY7	LG.3A10	Biolegend	124226
LY6C	APC-Fire 750	HK1.4	Biolegend	128026

Table S3: List of antibodies used in lineage depletion cocktail. (Related to experimental procedures)

Antigen	**Conjugation**	**Clone**	**Company**	**Catalog no**
B220	Biotin	RA3-6B2	eBioscience	13-0452-86
CD19	Biotin	MB19-1	eBioscience	13-0191-86
CD3e	Biotin	145-2C11	eBiosciences	13-0031-85
CD11b	Biotin	M1/70	eBioscience	13-0112-85
Gr-1	Biotin	RB6-8C5	eBioscience	13-5931-85
TER119	Biotin	Ter-119	eBioscience	13-5921-85

Table S4: List of antibodies used for live imaging of myeloid colonies. (Related to main figure 6)

Surface marker	**Conjuagte**	**Clone**	**Company**	**Catalog no**
CD115	PE	AFS98	eBioscience	12-1152-82
LY6G	BV480	1A8	BD Biosciences	746448
FCεR1	APC	MAR-1	eBioscience	17-5898-82

Table S5: List of antibodies for quantitative immunostaining of transcription factors. (Related to main figure 4)

Antigen	**Antibody**	**Dilution**	**Clone**	**Company**	**Catalog no**
GATA2	Rabbit anti-GATA2	1:50	H-116	SCBT	sc-9008
GATA1	Rat anti-GATA1	1:25	N6	SCBT	sc-265
FOG-1	Goat anti-FOG1	1:50	M-20	SCBT	sc-9361
PU.1	Rabbit anti-PU.1	1:50	T-21	SCBT	sc-352
CEBPα	Rabbit anti-CEBPα	1:50	14AA	SCBT	sc-61
IRF8	Goat anti-IRF8	1:50	C-19	SCBT	sc-6058
VENUS	chicken anti-GFP	1:1000	Polyclonal	Aves	GFP-1020
GATA2 (tissues)	rabbit anti-GATA2	1:200	Polyclonal	Novus	NBP1-82581

Secondary Antibody	**Conjugation**	**Dilution**	**Company**	**Catalog no**
Donkey anti-rabbit	Alexa 488	1:200	Invitrogen	A21206
Donkey anti-rat	Alexa 594	1:200	Invitrogen	A21209
Donkey anti-goat	Alexa 594	1:200	Invitrogen	A11058

Table S6: List of cytokines for culture of HSPCs. (Related to main figure 5 & 6)

Cytokine	**Concentration**	**Company**	**Catalog no**
SCF	100 ng/ml	Peprotech	250-03
EPO	2 units/ml	Peprotech	100-64
TPO	100 ng/ml	Peprotech	315-14
IL3	20 ng/ml	Peprotech	213-13
IL6	10 ng/ml	Peprotech	216-16
IL9	50 ng/ml	Peprotech	219-19
GM-CSF	20 ng/ml	Peprotech	AF-315-03

Table S7: List of filters used for imaging and quantification of transcription factor immunostainings. (Related to main figure 4)

Fluorophore	**Filter**	**Ex.spec**	**Em.spec**	**Beamsplitter**	**Company**	**Catalog no**
Alexa 488	EGFP ET	470/40	525/50	495 LP	AHF	F46-002
Alexa 594	mCherry	550/32	605/15	BS 585	AHF	F37-550 F38-585 F37-605
DAPI	DAPI	405/10	460/50	405 LPX	AHF	F39-404 F47-460 F48-404

Table S8: List of filters used for imaging of liquid culture colonies. (Related to main figure 6)

Fluorophore	**Filter**	**Ex.spec**	**Em.spec**	**Beamsplitter**	**Company**	**Catalog no**
GATA2VENUS	YFP ET	500/20	535/30	515 LP	AHF	F46-003
CD115-PE	mCherry	550/32	605/15	BS 585	AHF	F37-550 F38-585 F37-605
FCεR1-APC	Cy5	620/60	700/75	LPXR 660	AHF	F49-620 F48-660 F47-700
LY6G-BV480	CFP ET	436/20	480/40	455 LP	AHF	F46-001

Experimental procedures:

Generation of GATA2VENUS knock-in reporter mouse line:
The GATA2Venus knock-in construct consists of 5.0 *kbp* 5′-end homology arm lasting until the last codon of *Gata2* (skipping the endogenous stop-codon) followed by a 24 *bp*-short linker sequence (AGAGCATCAGGTACCAGTGGAGCT) encoding 8-amino acid peptide (Arg-Ala-Ser-Gly-Thr-Ser-Gly-Ala), the coding sequence of *Venus*, FRT (Flp recognition target)-flanked neomycin resistance gene cassette and 5 *kbp* 3′-end homology arm. Downstream of the 3′- homology arm there is a negative selection cassette consisting of herpes simplex virus thymidine kinase (HSV-TK) driven by the MC1 promoter. JM8.A3.N1 ES cells (C57BL/6J background) were electroporated (250 V, 500 µF; Gene Pulser Xcell, BioRad) with linear (*Gata2Venus*) construct followed by selection with 0.2 mg/ml G418 and 2 µM ganciclovir. 24 clones were picked, expanded and prepared for screening according to described protocols(Anastassiadis et al., 2013). Correct integration was confirmed in 9 clones by 5′- and 3′- end southern blot assay. In brief, genomic DNA was digested with HindIII (for 5′ end) or EcoRI (for 3′ end), separated on 0.8% agarose gels, blotted on nylon membranes (PALL) and hybridized with radioactively labeled (^{32}P-dCTP) by random priming (High Prime, Roche diagnostics) 5′- and 3′-probe respectively. Germline chimeras were generated from correct ES cell clone by ES-cell aggregation. Founders were identified by *Gata2Venus* PCR and FRT-flanked neo-selection cassette was excised *in vivo* using recombinase-mediated excision by crossing with Flpe deleter strain(Dymecki, 1996). Resulting GATA2VENUS offspring were backcrossed for >5 generations with C57BL/6J animals. Identification of homozygous *Gata2Venus* and wild-type animals was done by *Gata2Venus* specific genotyping protocol using the following set of primers: (a) *Gata2* forward primer: 5′- GAAGTCACCGCCCTTCAGTG -3′, (b) *Gata2* reverse primer: 5′- CTGCCAAACCACCCTTGATG -3′ and (c) *Venus* reverse primer: 5′- CGGACACGCTGAACTTGTGG -3′. *Gata2Venus* alleles is identified by a 290 bp band while wild-type *Gata2* allele by a 222 bp band.

Isolation of primary HSPCs:
Male mice for FACS analysis and HSPC isolation were euthanized at age of 12 – 16 weeks. Isolation of primary HSPCs was performed according to protocols described[27–37]. Briefly, femurs, tibiae, humeri and vertebrae of adult mice were isolated, crushed in FACS buffer (2% FCS (PAA) + 1mM EDTA (Invitrogen) in PBS (Sigma Aldrich)), subjected to ACK (Lonza) lysis buffer (for 2 min), lineage depletion using biotinylated antibodies (incubation for 15 min) followed by Streptavidin-conjugated beads (Roche) (incubation for 7 min) and immune-magnetic (Stem Cell Technologies) depletion (incubation for 7 min). Lineage depleted cells were finally stained with color-conjugated primary antibodies for 90 minutes on ice. FACS analysis and sorting was performed on FACS ARIA III (BD Biosciences).

Immunostaining of transcription factors in primary HSPCs:
Immunostaining of TFs in primary HSPCs was performed according to protocols as described(Etzrodt et al., 2018; Hoppe et al., 2016). Briefly, HSPCs were isolated, directly seeded on Poly-L Lysine (Sigma Aldrich) coated, plastic-bottom 384 well plates (Greiner Bio-one), stored for 30 min at 4°C, fixed with 4% paraformaldehyde (Sigma Aldrich) for 10 min at RT, washed thrice with PBS, permeabilized with PBS-T (0.2 % triton X (AppliChem) in PBS) for 5 min, washed twice with TBS-T (0.1 % Tween (Sigma Aldrich) in TBS buffer), incubated with blocking buffer (10 % donkey serum (Jackson Immuno research) in TBS-T) for 1h at RT, incubated with primary antibodies (1:50 dilution in blocking buffer) overnight at 4º C, washed thrice with blocking buffer, stained with secondary antibodies (1:200 dilution in blocking buffer) for 1h, incubated with DAPI (1:10000 in blocking buffer), washed thrice with blocking buffer, incubated with PBS and imaged. Images were acquired on a Nikon Eclipse Ti-E microscope using Lumencore light source with 0.7x camera adapter and 10X objective with 0.45 NA (Plan Apo) and analyzed using bioimaging pipeline described below.

Immunostaining of embryonic tissues:
The day of the vaginal plug was considered embryonic day (E) 0. Fresh isolated E14 embryos were immediately frozen, subsequently embedded on Optimal Cutting Temperature (OCT) (PolyFreeze, Sigma) and stored at -80°C until further processing. Full embryo cryosectioning (20 µm thick) was performed with a cryostat (CryoStar™ NX50 Cryostat, ThermoFisher) on superfrost glass slides, immediately fixed with 4% PFA for 20 min at room temperature and then stored in 1xPBS at 4°C. Tissue sections were immunostained with primary antibodies diluted in blocking solution (0.5% Triton-X in PBS with 10% NDS) overnight at 4°C. Sections were washed twice in PBS and fluorescent secondary antibodies were applied in blocking solution for 90 min at room temperature. DAPI was used to visualize nuclei. Sections were again washed two times and mounted in ProLong Diamond Antifade Mountant (ThermoFisher). Confocal images were taken on a Leica TCS SP5 equipped with three photomultiplier tubes, two HyD detectors, five lasers (405 nm, Argon Laser (458, 476, 488, 496 and 514 nm), 561, 594 and 633 nm) using 10X and 20x objective lens. All scans were acquired at 20–25 °C, 100 Hz, in the

bidirectional mode, with z-spacing of 0.3 - 1 μm at 1024x1024 pixel resolution. Images were acquired in 8-bit format.

Immunostaining of adult kidney:
Tissue preparation: Tissue sections were prepared as described before(Coutu et al., 2018). Bones were fixed for 24 hours in 4% PFA at 4º C. Kidneys were fixed for 1 hour in 4% PFA at room temperature. The tissues were embedded in 4% low-gelling temperature agarose and subsequently sectioned (100 μm thick) using a vibratome (Leica VT1200 S).
Immunostaining: All steps were performed at room temperature with gentle rocking in double side adhesive silicon chambers (Grace Biolabs) glued on glass slides. Sections were blocked and permeabilized with TBS (final concentration 0.1M Tris, 0.15 M NaCl, pH 7.5) containing 0.05% Tween-20, 20% DMSO, 1% Triton X 100 and 10% donkey serum (Jackson Immuno Research) for a minimum of 2 hours. This buffer was also used to dilute all primary and secondary antibodies. Primary antibodies were applied overnight. Secondary antibodies were applied for 2 hours. After extensive washing (with TBS-T), sections were mounted in homemade mounting medium (80% Glycerol in TBS containing 0.2 M N-propyl gallate, pH 8.5) using size 1.5 coverslips.
Confocal microscopy: Confocal microscopy was performed on a Leica TCS SP8 equipped with three photomultiplier tubes, two HyD detectors, five lasers (405 nm, Argon Laser (458, 476, 488, 496 and 514 nm), 561, 594 and 633 nm) using Leica type G immersion liquid and a 63x glycerol immersion lens (NA 1.3, FWD 0.28 mm). All scans were acquired at 20–25 °C, 400 Hz, in the bidirectional mode, with z-spacing of 1 μm (the optical slice thickness of the optics was 0.99 μm) at 1024x1024 pixel resolution. Images were acquired in 8-bit format. For signal acquisition only HyD detectors were used.

Protein stability assay of transcription factors:
HSPCs were sorted (described above) and cultured in plastic-bottom 384 well plates in multi-lineage supporting media (IMDM (Gibco) + 5 % BIT + P/S (Gibco) + SCF + EPO + TPO + IL3 + IL6). Cells were treated with 50 μM cyclohexamide (Sigma Aldrich) for indicated time duration, fixed immediately with 4% paraformaldehyde (Sigma Aldrich) and proceeded with standard immunostaining protocol (described above)(Hoppe et al., 2016).

Single-cell liquid culture colony assay of HSPCs:
HSPCs were single-cell sorted in plastic-bottom 384 well plates (Greiner Bio-one) using FACS ARIA III with pan myeloid culture media as described (IMDM (Gibco) + 5 % BIT (Stem Cell Technologies) + 10% FCS (PAA) + P/S (Gibco) + SCF + GM-CSF + IL3 + IL9)(Drissen et al., 2016). Plates were incubated at 37° C and 5% CO2. At day 8, color-conjugated antibodies against lineage markers were added (1:5000) to wells, incubated for 3 hours at 37°C and 5% CO2 and imaged. Images were acquired on a Nikon Eclipse Ti-E microscope using Lumencore light source with 0.7x camera adapter and 10X objective with 0.45 NA (Plan Apo) and analyzed as described below.

FACS analysis of bulk-liquid culture colonies:
HSPCs were sorted using FACS ARIA III and 100 – 200 cells were seeded in each well of 24 well plates (Thermo scientific) with pan myeloid media (described above). Plates were incubated at 37° C and 5% CO2. At day 8, cells were taken, washed with FACS buffer (2% FCS in PBS), stained with color-conjugated antibodies against lineage markers, incubated for 90 min at 4°C and washed with FACS buffer. Finally, FACS analysis of cell types was performed using FACS ARIA III.

May-Grünwald and Giemsa staining of mature colonies:
May-Grünwald and Giemsa staining was performed according to protocol as described (Hettich). Briefly, cytospin hardware was arranged and 200 μl of cells were taken directly from day 8 culture of HSPCs and added on cytospin columns. Cells were centrifuged at 270g for 3 minutes. Supernatant was removed carefully followed by second round of centrifugation at 270g for 1 minute. Air dried the slides and 1 ml of May-Grünwald (Roth) solution was added for 4 minutes. Slides were washed twice with dist. H2O and 1 ml of 5% Giemsa solution (Sigma Aldrich) was added for 16 minutes. Slides were washed twice with dist. H2O. Air-dried the slides followed by imaging. All steps were performed at 4º C. Images were acquired using Nikon Eclipse Ti-E microscope.

Bioimaging pipeline for image acquisition, detection and quantification:
Fluorescence images (immunostaining of transcription factors and single-cell liquid colony assays) were acquired on Nikon Eclipse Ti-E microscope in an automated manner using custom written software. Single-cell colonies were analyzed based on fluorescence signal of surface markers and scored manually. To count the number of cells per colony, cells were segmented in brightfield based on morphology and quantified using FastER segmentation tool(Hilsenbeck et al., 2017). To quantify the signal of transcription factors in single cells, background signal was normalized by using BaSiC tool as previously described(Peng et al., 2017) and segmentation of cells was

performed on DAPI signal. Finally, quantification of transcription factor signal was performed using fastER segmentation tool as described(Hilsenbeck et al., 2017). Data was analyzed using custom written R scripts.

References:

Anastassiadis, K., Schnütgen, F., von Melchner, H., and Stewart, A.F. (2013). Gene Targeting and Site-Specific Recombination in Mouse ES Cells. Methods Enzymol. *533*, 133–155.
Arinobu, Y., Iwasaki, H., Gurish, M.F., Mizuno, S., Shigematsu, H., Ozawa, H., Tenen, D.G., Austen, K.F., and Akashi, K. (2005). Developmental checkpoints of basophil/mast cell lineages in adult murine hematopoiesis. *102*, 1–6.
Cabezas-Wallscheid, N., Klimmeck, D., Hansson, J., Lipka, D.B., Reyes, A., Wang, Q., Weichenhan, D., Lier, A., Von Paleske, L., Renders, S., et al. (2014). Identification of regulatory networks in HSCs and their immediate progeny via integrated proteome, transcriptome, and DNA methylome analysis. Cell Stem Cell *15*, 507–522.
Chen, C.-C., Grimbaldeston, M.A., Tsai, M., Weissman, I.L., and Galli, S.J. (2005). Identification of mast cell progenitors in adult mice. Proc. Natl. Acad. Sci. *102*, 11408–11413.
Coutu, D.L., Kokkaliaris, K.D., Kunz, L., and Schroeder, T. (2018). Multicolor quantitative confocal imaging cytometry. Nat. Methods *15*, 39–46.
Drissen, R., Buza-Vidas, N., Woll, P., Thongjuea, S., Gambardella, A., Giustacchini, A., Mancini, E., Zriwil, A., Lutteropp, M., Grover, A., et al. (2016). Distinct myeloid progenitor-differentiation pathways identified through single-cell RNA sequencing. Nat. Immunol. *17*, 666–676.
Dymecki, S.M. (1996). Flp recombinase promotes site-specific DNA recombination in embryonic stem cells and transgenic mice. Proc. Natl. Acad. Sci. *93*, 6191–6196.
Etzrodt, M., Ahmed, N., Hoppe, P.S., Loeffler, D., Skylaki, S., Hilsenbeck, O., Kokkaliaris, K.D., Kaltenbach, H.-M., Stelling, J., Nerlov, C., et al. (2018). Inflammatory signals directly instruct PU.1 in HSCs via TNF. Blood blood-2018-02-832998.
Hettinger, J., Richards, D.M., Hansson, J., Barra, M.M., Joschko, A.C., Krijgsveld, J., and Feuerer, M. (2013). Origin of monocytes and macrophages in a committed progenitor. Nat. Immunol. *14*, 821–830.
Hilsenbeck, O., Schwarzfischer, M., Loeffler, Di., DImopoulos, S., Hastreiter, S., Marr, C., Theis, F.J., and Schroeder, T. (2017). FastER: A User-Friendly tool for ultrafast and robust cell segmentation in large-scale microscopy. Bioinformatics *33*, 2020–2028.
Hoppe, P.S., Schwarzfischer, M., Loeffler, D., Kokkaliaris, K.D., Hilsenbeck, O., Moritz, N., Endele, M., Filipczyk, A., Gambardella, A., Ahmed, N., et al. (2016). Early myeloid lineage choice is not initiated by random PU.1 to GATA1 protein ratios. Nature *535*, 299–302.
Iwasaki, H., Mizuno, S., Mayfield, R., Shigematsu, H., Arinobu, Y., Seed, B., Gurish, M.F., Takatsu, K., and Akashi, K. (2005). Identification of eosinophil lineage–committed progenitors in the murine bone marrow. J. Exp. Med. *201*, 1891–1897.
Kiel, M.J., Yilmaz, O.H., Iwashita, T., Yilmaz, O.H., Terhorst, C., and Morrison, S.J. (2005). SLAM family receptors distinguish hematopoietic stem and progenitor cells and reveal endothelial niches for stem cells. Cell *121*, 1109–1121.
Peng, T., Thorn, K., Schroeder, T., Wang, L., Theis, F.J., Marr, C., and Navab, N. (2017). A BaSiC tool for background and shading correction of optical microscopy images. Nat. Commun. *8*, 1–7.
Pop, R., Shearstone, J.R., Shen, Q., Liu, Y., Hallstrom, K., Koulnis, M., Gribnau, J., and Socolovsky, M. (2010). A key commitment step in erythropoiesis is synchronized with the cell cycle clock through mutual inhibition between PU.1 and S-phase progression. PLoS Biol. *8*.
Pronk, C.J.H., Rossi, D.J., Månsson, R., Attema, J.L., Norddahl, G.L., Chan, C.K.F., Sigvardsson, M., Weissman, I.L., and Bryder, D. (2007). Elucidation of the Phenotypic, Functional, and Molecular Topography of a Myeloerythroid Progenitor Cell Hierarchy. Cell Stem Cell *1*, 428–442.
Qi, X., Hong, J., Chaves, L., Zhuang, Y., Chen, Y., Wang, D., Chabon, J., Graham, B., Ohmori, K., Li, Y., et al. (2013). Antagonistic Regulation by the Transcription Factors C/EBPα and MITF Specifies Basophil and Mast Cell Fates. Immunity *39*, 97–110.
Wilson, A., Laurenti, E., Oser, G., van der Wath, R.C., Blanco-Bose, W., Jaworski, M., Offner, S., Dunant, C.F., Eshkind, L., Bockamp, E., et al. (2008). Hematopoietic Stem Cells Reversibly Switch from Dormancy to Self-Renewal during Homeostasis and Repair. Cell *135*, 1118–1129.
Yanez, A., Ng, M.Y., Hassanzadeh-kiabi, N., and Goodridge, H.S. (2017). IRF8 acts in lineage-committed rather than oligopotent progenitors to control neutrophil vs monocyte production. *125*, 1452–1460.